Quality Research, Development, and Consulting Inc.

SMART SCREENING SYSTEM (S3)

IN TACONITE PROCESSING

FINAL REPORT

Department Of Energy (DOE)
Report Start Date: Sep. 09, 2002
Report End Date: Sep. 08, 2006
Principle Investigator: Dr. Daryoush Allaei
Report Issued Date: Dec. 20, 2006
DOE Award # DE-FC26-02NT41470

Q.R.D.C., Inc.
PO Box 562, Excelsior, MN 55331

Smart Screening System (S3) In Taconite Processing

Final Report

This report is prepared for

Department Of Energy (DOE) & Partners
(Partners include: Albany Research Center, ISPAT Inland Mining,
U.S. Steel-Minntac, and S3i)

DOE Award # DE-FC26-02NT41470
Report Issued Date: Dec. 20, 2006

Report Author
Dr. Daryoush Allaei, P.E.
Ryan Wartman

Report Editors
Mr. Asim Syed Mohammed
Mr. David Tarnowski

Any questions or comments regarding this report
should be directed to the principle investigator

Disclaimer

ACKNOWLEDGMENT

This Final report titled “Smart Screening System (S3) In Taconite Processing” was prepared with the support of the U.S. Department of Energy, under Award No. DE-FC26-02NT41470. However, any opinions, findings, conclusions, or recommendations expressed herein are those of the author(s) and do not necessarily reflect the views of the DOE.

ABSTRACT

The conventional screening machines used in processing plants have had undesirable high noise and vibration levels. They also have had unsatisfactorily low screening efficiency, high energy consumption, high maintenance cost, low productivity, and poor worker safety. These conventional vibrating machines have been used in almost every processing plant. Most of the current material separation technology uses heavy and inefficient electric motors with an unbalanced rotating mass to generate the shaking. In addition to being excessively noisy, inefficient, and high-maintenance, these vibrating machines are often the bottleneck in the entire process. Furthermore, these motors, along with the vibrating machines and supporting structure, shake other machines and structures in the vicinity. The latter increases maintenance costs while reducing worker health and safety.

The conventional vibrating fine screens at taconite processing plants have had the same problems as those listed above. This has resulted in lower screening efficiency, higher energy and maintenance cost, and lower productivity and workers safety concerns. The focus of this work is on the design of a high performance screening machine suitable for taconite processing plants.

SmartScreens™ technology uses miniaturized motors, based on smart materials, to generate the shaking. The underlying technologies are Energy Flow Control™ and Vibration Control by Confinement™. These concepts are used to direct energy flow and confine energy efficiently and effectively to the screen function. The SmartScreens™ technology addresses problems related to noise and vibration, screening efficiency, productivity, and maintenance cost and worker safety. Successful development of SmartScreens™ technology will bring drastic changes to the screening and physical separation industry.

The final designs for key components of the SmartScreens™ have been developed. The key components include smart motor and associated electronics, resonators, and supporting structural elements. It is shown that the smart motors have an acceptable life and performance. Resonator (or motion amplifier) designs are selected based on the final system requirement and vibration characteristics. All the components for a fully functional prototype are fabricated and have been tested.

TABLE OF CONTENTS

LIST OF FIGURES

EXECUTIVE SUMMARY

Two undesired components of the material processing industry are excessive consumption of energy and extreme noise and vibration. Current screening machines use an electrical motor with a rotating unbalanced mass to generate shaking. These motors not only generate motion in the screen panels but also shake the supporting structures and other machines and structures in a plant. During initial field investigations of existing screening machines, it was found that the existing vibrating screens are inefficient, noisy, and waste significant amounts of energy. Many areas were identified that need either improvement or a complete changeover. These areas include: material handling; screening process; screen blinding; moving mass; motion; energy consumption; noise levels; vibration transmission; and workers' safety.

To address the above-mentioned issues, QRDC proposed an innovative concept, SmartScreens™ technology, based on smart materials (miniaturized motors), and Energy Confinement and Flow Control. This project is jointly funded by the DOE and industry partners that include representatives of the mining industry ISPAT INLAND MINING, U.S. Steel-MINNTAC (Minnesota ore operations), QRDC (a technology company with an extensive relevant track record), S3i (screen manufacturing company transferring the prototypes to full marketable and producible products), and the Albany Research Center (provide solutions that makes national energy systems safe, efficient, and secure). The key objective of this project was to demonstrate the feasibility of energy management-based SmartScreens™ that can efficiently handle and process material separation. SmartScreens™ have the capability to control the flow of energy and confine this energy to the screen itself rather than shaking the entire machine and the surrounding structure, which comprises conventional vibratory screening machines. Better control of energy flow results in better screen recovery and reduced re-circulating load of the slurry. Single or multi-stage resonators with an advanced sensory system can be used to continuously monitor screening processes to improve productivity. Smart material-based miniaturized motors offer better control over speed of operation, and the type/magnitude of motion. These abilities help to effectively clean the screens and avoid blockage or blinding of the screens. Miniaturized motors eliminate any moving components such as bearings and a bulky unbalanced rotating mass. This, in turn, virtually eliminates noise. With the proposed SmartScreens™ technology, the weight of the moving mass can be reduced by as much as 80%, resulting in a significant energy usage reduction.

In the development efforts of SmartScreens™, baseline data was obtained and an initial field investigation was completed to identify problem areas in the current fine screens. Based on this information, a plan was developed that identified the basic design requirements to improve and efficiently handle the screening process. Various conceptual designs were identified for the key components of the system. These key component designs (i.e., smart motor and motion amplifiers or resonators) were modeled in CAD programs and analyzed through computer simulation and experimental tests. Some of the key component designs were selected and a full system was modeled that included the screen panel, four resonators, miniaturized smart motors, and the supporting structure for

resonators and screen panel. The performance of these key components and systems was analyzed under various loading conditions through finite element analysis and experimental tests. Based on these results, three systems were selected. After a detailed review, one or two of these key components and systems were fabricated as a prototype for the SmartScreen™.

The SmartScreens™ technology, with its capabilities to reduce current energy requirements, reduce maintenance costs in screening operations, improve throughput, and reduce noise and vibrations levels, can impact the global process industries. The widespread application of the proposed technology could change the way material separation is handled in general processing industries. Candidate industries are oil and gas, mineral processing, food processing, and pharmaceutical applications.

INTRODUCTION

Current screening machines have one thing in common: they operate using an electrical motor with a rotating unbalanced mass to generate shaking. Based on the information from Minntac Grant Application [1], Minntac has struggled with finding engineering solutions for noise and vibration problems caused by conventional screening machines. Evaluations of isolation curtains/walls, different screening machine brands, and lower speeds have resulted in minimal improvements in noise levels and have significantly compromised production. Blinding of screens is another major cause for loss in production. Minntac has estimated that approximately 2494 megawatt hours per year alone are lost due to poor screening recovery and wasted energy.

The ultimate goal of this project was to develop SmartScreens™ that will replace the inefficient massive electric motors. SmartScreens™ will have miniaturized smart motors (ceramic- or electromagnet-based). SmartScreens™ will incorporate an energy management technique to control energy flow and will confine injected shaking energy to the screen panels. In 2002, the QRDC team proposed to combine state-of-the-art smart materials, the concept of single or multi-stage resonators, and the patented energy management technique. This innovative technology has won several Research and Development awards from the U.S. Army, Navy, and Air Force and commercial organizations [2-6].

Previous reports have shown through computer simulations and laboratory prototypes that smart motors, accompanied by specially designed resonators, meet current screening vibration levels while simultaneously significantly reducing power consumption and energy loss. The ceramic materials and electromagnetic drives used in these motors are well suited for applying large dynamic forces and the required shaking functions to resonators. The smart motors consume 50% to 96% less energy than the bulky electrical motors, and are capable of operating over a wide range of frequencies. They are almost maintenance free, as they do not have any moving components and do not need lubrication. Additionally, smart materials (such as PZTs) can function as both collocated sensors and actuators for active control of the shaking action and process automation.

The ultimate goal of this project is to develop SmartScreens™ that will replace the inefficient massive electric motors. SmartScreens™ will have miniaturized, ceramic-based smart motors. SmartScreens™ will incorporate an energy management technique to control energy flow and will confine injected shaking energy to the screen panels. As part of the development efforts of SmartScreens™, a Steering Committee for Smart Screen Systems (SC-S3) was formed. Members of SC-S3 are QRDC (leading role), ARC (Albany Research Center, provide solutions that makes National's energy systems safe, efficient, and secure), U.S. Steel-MINNTAC (Minnesota ore operations), Ispat Inland Mining, S3i (Smart Screen System Inc.), and a representative of DOE-NETL. The QRDC team proposed to combine state-of-the-art smart materials, the concept of single or multi-stage resonators, and QRDC's recently patented energy management technique. This innovative technology has won several Research and Development awards from the U.S. Army, Navy, and Air Force and commercial organizations [2-4].

A miniaturized motor consumes 96% less energy than the bulky electrical motors and is capable of operating over a wide range of frequencies. Even when multiple smart motors are used to run the system, energy saving per system is significant. These motors are almost maintenance free as they do not have any moving components and do not need lubrication. Piezoelectric ceramic material (Such as PMN= Lead Magnesium Niobate, and PZT=Lead Zirconate Titanate) can be miniaturized. Ceramic materials are well suited for applying large dynamic forces and the required shaking functions to resonators. In addition, ceramic materials can function as collocated sensors and actuators for active control of the shaking action and process automation. Cantilever resonators of appropriate shape and size are used as resonators to amplify the displacements and accelerations so that the screening function is optimized. The combination of resonators and smart materials offers full control and precision of the shaking function. Finally, the system has been optimized by incorporating the energy management techniques that have been developed by QRDC. It is the combination of smart materials and the vibration energy-managing method that makes the approach unique and innovative. Energy management is composed of energy diversion, confinement, dissipation, conversion, and cancellation.

The proposed technology offers significantly better energy management by controlling the flow of energy and confining it to screen panels rather than shaking the supporting frame, motor and surrounding structure. SmartScreens™ offer better control over the speed of operation, and type and magnitude of motion. These abilities help to quickly clean the screens and avoid blockage or blinding of screens. By using miniaturized motors to focus energy, SmartScreens™ eliminate and/or downsize many of the structural components typically associated with industrial screens. As a result, the screening or processing surface area of the machine increases for a given footprint and space envelope. This increase in usable screening surface area extends the life of the screens and reduces required maintenance. Energy management and better control of the screening process helps to remove particles of the correct size and thus increase the throughput, reduce material re-circulation, and significantly reduce power consumption.

The primary objectives of this project include: 1) designing a screening system for the taconite mining industry with an alternative, low energy, driving mechanism; 2) fabricating the system for installation into an actual plant; 3) testing the device in multiple processing environments; and, 4) refining the design to make the product a feasible industry option. All of these objectives have been met by QRDC, and in some cases these goals have been exceeded. The design includes a PZT-powered screening system that consumes a small part of the energy of a classical screening unit. A system was fabricated and tested, showing vibration levels, sound levels, operating speeds, and screening efficiencies to be as good as or better than predicted performance. Testing of the fabricated unit was performed in multiple plants around the mid-West, on multiple occasions. Finally, refinements were made to the system for adaptation to the real marketplace, both in the field of taconite and the seed cleaning industry.

This report summarizes the entire work that has been done since the start of this DOE funded project in September of 2002. Chapters 1 and 2 focus on the development of Smart Screens for the taconite mining industry, both design and testing, respectively. Chapters 3

and 4 detail the results of the continuation of the project into the dry application (or seed cleaning) industry, again covering both design and testing results, respectively. This continuation was due to the immediate promise of Smart Screen technology in other industries, and was awarded by the DOE in September 2005. The last chapter states the conclusions made by QRDC in regard to the project and its successes.

CHAPTER I – TACONITE SYSTEM DESIGN & ANALYSIS

During the first months of the project, fine screens at Minntac were examined to quantify efficiency and problem areas currently in the field. Noise and vibration data was collected on screens and structures in the vicinity of the screens. During this data collection and assessment session, noise levels as high as 107 dBA were recorded. It was also found that these machines waste much of their energy due to useless elastic deformation of the heavy supporting structures. Audible and very loud noise and excess heat were also of concern. The latter causes the moving components, such as bearings, to have a reduced useful life, thus creating excess maintenance cost for a processing plant. Current fine screens do not have control of energy flow and cannot confine the energy to the screening area itself (mesh). Due to this limitation, large masses of the machines are vibrated to achieve material separation, and cause massive vibration transmission to other machines and structures in the vicinity.

S3I's SmartScreens™ are comprised of three primary components. These components are: smart motor, resonator, and supporting structure. What follows in this chapter are descriptions of what steps were taken in the design refinements, and what analyses were performed before fabrication and testing took place.

1.1 The Smart Motor

Two types of ceramic-based smart motor designs were developed by the QRDC team. An overview of these designs is presented in this section. A detailed description of the designs is presented in Appendix A.

Both motor assemblies share the same basic components. The piezoelectric (PZT) ceramic is one of the key components of the motor. The PZT element expands and contracts with an increase and decrease in voltage, respectively. These PZT actuators are made of Lead Zirconate Titanate (PZT) in the shape of small discs stacked on top of one another, as shown in Figure 1.1. PZT actuators have unique features. They expand when an electrical potential (voltage) is placed over the top and bottom opposing surfaces. They can provide a tremendous amount of force from a relatively small amount of voltage. Finally, their reactions are near instantaneous to their voltage inputs. These three attributes make them very attractive for the smart motor designs, which require large forces with small power requirements and good frequency control.

There were two primary challenges that needed to be addressed when designing the PZT actuators for this application. First, the displacement output (stroke) of a PZT actuator is so small that it is expressed in microns. Second, ceramic-based actuators are brittle and easy to fracture. These two challenges are the main reasons that additional smart motor components are required in the overall assemblage of the motor. Mechanical amplifiers or resonators serve the purpose of amplifying the PZT stroke. The force transfer component serves as the main device to connect the resonator to the PZT actuator, and thereby excites a system mode that will transfer energy more efficiently to the screen panel. Since shear loads and friction are detrimental to the ceramic and limit system performance, uniform loading and minimal friction losses are required. Also, since the ceramic applies force only in the extension

direction, preload and restoring components are needed. Additional details on these motor components are included in Appendix A.

In addition to the above-mentioned components, the final smart motor design includes three important design parameters: 1) an easy ceramic installation that requires no adhesive; 2) only one preload required; and, 3) large holes are incorporated for wires. This design is detailed in Appendix A.

1.1.2 Oscillating Mass Design

Another design approach, the oscillating mass design, was considered as an alternative to base excitation. The approach is based on the idea that single or multiple oscillating masses could be actively excited at their natural frequencies (similar to the resonator designs), and the resonators underneath the live deck could be passive and part of the supporting structure. The details of the designs investigated are presented in Appendix A.

1.2 Resonators

Resonators (or motion amplifiers) are another key component of the screening system. A resonator is designed to have two functions. First, it amplifies the displacement of a smart motor and delivers motion to the screen (panel). Second, it creates a vibratory motion that provides motion to the screen in both vertical and flow directions. One example of resonator design iteration is shown in Figure 1.2. These resonator designs are comprised of single and split curve resonator. Using finite element modeling (FEM), it was determined that the split resonator concept generates acceptable stress levels when subjected to excitation.

1.2.1 Resonator Fatigue Life

Further refinements were performed to reduce the stress levels and to better distribute stresses on the curved section of resonator. Production units with magnetic motors were used for the analysis purpose and the performance was analyzed by varying resonator geometry. The key objective of this study was to optimize resonator shape to reduce stress levels on the resonators. Two main cases were analyzed: one with reduced thickness at the center of the resonator; and another with varying width of the resonator at the center away from straight section. Forced vibration analysis results showed 10% drop in resonator stress levels by reducing width at the center of the resonator while reducing thickness raised stress levels.

1.2.1.1 Analysis details

A current production unit is shown in Figure 1.3, and its results were used as a baseline. Solid models of the resonator were created in SolidWorks and then transferred to ANSYS. Some constraints taken into consideration during resonator optimization process were:

1. Operating mode frequency should be maintained at or above 45 Hz.
2. Height of the resonator should remain the same, with a maximum tolerance of 1/8”.
3. Width of the resonator should remain 3.5” on the top portion, and 4” on the bottom.

The following two cases were analyzed to evaluate stress levels and distribution on the resonator under forced vibration. Input and reaction forces were applied on feed end resonators and motor mounting blocks respectively to simulate magnetic motor force inputs.

- **Case 1**: Varying resonator width at the center along the curved portion while maintaining same width at the top and bottom end straight section. Total six different resonator geometries were analyzed starting with 1 inch width at the resonator center and increasing width in steps of 0.5 inch. Figure 1.4 shows two out of six extreme cases.
- **Case 2**: Effect of varying resonator thickness along the curved section with tapered from both straight section and going to minimum at the center as shown in Figure 1.5.

For all cases, vibration data was collected at six points on the panel and resonator stresses were calculated only after matching average displacement.

1.2.1.2 Analysis Results for Case 1

The current system with a 3" wide resonator at the center was used as the baseline and one of the six cases. Analysis results showed some improvement in system performance and around 10% drop in stress levels at feed end resonator. Figures 1.6 and 1.7 compare displacement on the panel at the front end for all six different cases with varying resonator width. It is clear from the figures that the operating mode frequency drops gradually with decreasing width. However, the system performance increases by 50% in the vertical direction at the discharge end, while the performance remains almost the same at the feed end in both directions. To calculate stress levels, force was dropped by 5% for most of the cases to match displacement with the baseline model as explained above. Figure 1.8 compares stress levels on right side upper and lower resonator for all cases. Figure 1.9 shows stress levels and distribution on resonator for extreme case and it is clear from the results that minimum width at the center of resonator will help reduce stress levels. Also, stress distribution for the resonator with 1-inch width at the center is much better, and the high stress area shifts from the top and bottom end towards the center of the resonator.

1.2.1.3 Analysis Results for Case 2

Thickness was gradually reduced to 0.195" at the center of the resonator starting with 0.375" on both ends. Force analysis results of this configuration did not help in any improvement in terms of stress levels and system performance, instead 20% more force was required to match the average displacement with that of baseline. Figure 1.10 compares stress levels on the resonator for baseline model and modified case.

1.2.2 Performance Improvement

Through finite element analysis, further attempts were made to improve system performance. Resonator dimensions (thickness and length) were used as the design parameters since the stroke generated by the smart motor is amplified through the resonator. The key objective of this study was to improve displacement amplification through resonator design. Along with the baseline case, three different cases were analyzed. For the first case, the resonator thickness was changed to the most extreme possible scenario that can be easily fabricated. The length was maintained at the same as the original resonator length. In the next two cases, the length along the straight portion was changed to bring the target mode frequency close to the baseline model. Analysis results did not show any further improvement.

1.3 Supporting Structure

For the screening system's supporting structure, QRDC engineers focused on a design that utilized tubular beams, as seen in Figure 1.11. This design adds support to the edges of the beams, reducing vibration levels and thus improving overall system performance. Simulated displacement results of the screen's surface (live deck) are shown for each case in Figure 1.12. The higher displacement at system operating frequency (~50Hz) for the tubular structure is compared to the original I-frame supports. It is observed that the maximum displacement is increased by about 75% on output end of the machine with slight improvement at feed end. This anticipated increase in performance was the key reason for the use of tubular beams in the supporting structure.

One of the most significant changes made to the supporting structure design involved completely removing the static plate, as shown in Figure 1.13. The initial purpose of the static plate was to allow for a connection interface between the vertical supporting legs and the resonator/motor assemblies. However, it was identified that this static plate introduces a number of issues and challenges, such as:

1) *Vibratory Energy Transmission to the Supporting Structure:* The resonators are mounted on the static plate, which in turn is mounted on relatively soft supporting structure, allowing vibration transmission to the legs and base.
2) *Static Plate Bending:* Due to its own weight and the soft supporting structure, the static plate has bending characteristics that add to the vibrations of the system. These excess vibrations are undesirable and could be detrimental to the life of resonators.
3) *Energy Loss through Extra Bolt Requirement:* Possibly the biggest issue is the 40 plus bolts required between the live deck and the supporting structure. As a result, the presence of the static plate negatively influences system performance, installation time, and maintenance cost.

A new support design, with no static plate, was developed. It should be noted that the number of nuts and bolts used in each design are substantially different. In the design with a static plate, approximately 100 nuts and bolts were used. With the newer design, shown in Figure 1.13, the number of bolts is cut in half due to removal of the static plate. Welding the legs to the base further reduced the number of bolts to around 25% of the other design. Additional bolts add not only time and effort to the assembly, but are also large sources for vibration and energy loss that could otherwise be used to excite the live deck.

1.4 PZT-Based System Isolation

The SmartScreen^{TM} system performance depends on installation conditions, as PZT-based smart motors need a rigid structure to push against in order to efficiently direct the energy to a moving mass. Since the stroke generated by ceramics is very small, any movement in the supporting structure will cause a drop in overall system performance. This problem can be addressed through different ways, such as: use of an oscillating mass (OM) driver; different mode excitation; system isolation from foundation; feeding energy back into the moving mass; displacement input instead of force input; and over-powering the system to

compensate for any losses. In this section, finite element analysis results of an isolation mount and different mode excitation is discussed.

1.4.1 Analysis Details

The PZT system as shown in Figure 1.14 was used to analyze effects of an isolation mount on system performance. ANSYS 8.0 was used for this analysis and mode superposition method was used for forced analysis. A fixed system without an isolation mount was analyzed and the results were used for baseline information. The system was then modified and four springs were added on each corner to closely represent a coil spring surface contact. Additional boundary conditions were added to avoid rigid body modes that could not be eliminated through four springs on each corner (see figure 1.14). Various spring rates were evaluated for the isolation mount, along with a fixed system (baseline), and the system response was analyzed under forced vibration. By adding the isolation mount, many modes were introduced and the target in-phase mode got complex due to contribution from the closely spaced modes. However, the out-of-phase mode between the livedeck and the supporting structure responded well to the input forces at the root of the resonators. The same input force magnitude of 1,000 lbs was maintained in all cases, and vibration data was collected at six points on the panel and two points on the solid frame. The following are the extreme cases that were analyzed and compared with baseline model:

Test 1: Same as baseline except 4 springs with a spring rate of 125 lb/in each were added on all four corners between supporting structure and base supporting structure.

Test 2: Same as Test 1 except a spring rate of 12500 lb/in for each spring was used.

Based on Test 1 & Test 2 analysis results, a parametric study was done to minimize motion on the supporting structure. It was assumed that increasing the mass of the supporting structure could reduce motion on the structure and improve overall system performance. For a quick analysis, the mass of the supporting structure was changed through material property (density). Three cases were analyzed by adding 2, 4 & 6 times the current mass of supporting structure, such that the resultant mass of supporting structure was 400 lb, 800 lb, 1600 lb & 2400 lb for baseline and rest of the cases, respectively.

Using the Test 1 system, another parametric study was done to analyze the influence of plant structure stiffness on system performance while operating in an out-of-phase mode. Beam elements with I-cross sections were used to quickly and efficiently model the plant structure. The plant structure was tuned to different frequencies (6, 11 & 15Hz) by changing overall height of the structure for parametric study.

1.4.2 Analysis Results

Baseline modal analysis resulted in an operating modal frequency of 49Hz. Based on a constant input force, a maximum displacement of 26 $mils_{pk\text{-}pk}$ was measured at the feed end and around 10 $mils_{pk\text{-}pk}$ at discharge end in vertical direction. In the horizontal direction, 65 $mils_{pk\text{-}pk}$ was measured on both ends. Motion on the solid frame was very minimal (below 3 $mils_{pk\text{-}pk}$) in both vertical and horizontal direction.

Test 1 resulted in many low frequency modes and the target mode was suppressed/got complex due to contribution of other modes. However, forced vibration analysis resulted in

decent system performance at a higher order mode (i.e., out-of-phase mode between the livedeck and the supporting structure at around 61Hz). Motion distribution on the panel at this mode reversed when compared to the baseline model, resulting in more motion on the discharge end and less motion on the feed end. The maximum displacement in the vertical direction almost remained the same as the baseline model, while the motion in horizontal direction dropped by 50%. This case also resulted in significantly larger motion on the supporting structure in the vertical direction that was close to 50% of the motion on the panel.

Test 2 results were similar to Test 1, except that the out-of-phase mode natural frequency changed to 65Hz, and the system performance dropped slightly. Figures 1.15 and 1.16 show the combined results of the above three cases in the vertical and horizontal directions, respectively, measured at the center of the rear and front end of the panel.

Figure 1.17 and Figure 1.18 show results of the solid frame mass parametric study. The results clearly show increasing solid frame mass will not reduce motion on the solid frame. In fact, it could increase the motion and drop system performance at the livedeck level.

The addition of a plant structure below the system did not affect the system performance while operating at the out-of-phase mode. Figure 1.19 shows the basic model and Figures 1.20 and 1.21 show force analysis results of the baseline model without a plant structure and with a plant structure of varying structural stiffness.

CHAPTER II – TACONITE SYSTEM TESTING & RESULTS

The final PZT system proved to be the best solution and exceeded performance expectation. Use of solid leg structure and coil springs to isolate system from the installation resulted in substantial increase in system performance. This design concept is referred to as the Suspended Solid Leg PZT system, or SSL-PZT system, and can be viewed in Figure 2.1.

In this chapter, a summary of the numerical and test results on the SSL-PZT system and key components are presented. The details of each test that include: supporting structure evaluation; full system performance in lab and field; longevity test of smart motor; dynamic force measurement of the smart motor; and, stress/strain measurement are presented. Issues, challenges, and recommended improvements are discussed. A brief discussion on the selection of the required materials for the production unit and the electrical equipment for controlling the PZT-based smart motor is also presented.

2.1 Supporting Structure Evaluation

The supporting structure on which the resonator and smart motor were mounted was redesigned to improve overall system performance. The key objective of this effort was to reduce structural vibration, retrofit a magnetic/smart motor, and eliminate soft structures (i.e. static plate & legs, refer to Figure 2.2). Some of the improvements of this new supporting structure design were:

- Single member design that eliminates need of static plate, most of the attachment, nuts and bolts and various fabrication processes.
- Improves system performance by reducing losses between various interfaces and structure deformation.
- Improves overall rigidity of the system and provides better coupling between each resonator.
- Improves fatigue life of resonators by minimizing resonator rotation due to undesired supporting structure deformation.
- Requires less time for assembly and minimizes maintenance cost.

As shown in Figure 2.1, the supporting structure was designed to directly mount to the resonator and the PZT-based Smart Motor assembly on the structure without any additional interface. The resonator and PZT-based smart motor mounting block, which is an integral part of the supporting structure, was designed to fit both magnetic motors and PZT-based smart motor. This design allows for independent installation of the smart motor and resonator and uses only two bolts to mount the smart motor. It requires less than 5 minutes for changing the smart motor by one person. This modified structure was much stiffer than the old supporting structure and the natural frequency of the first mode was above 200 Hz (refer Figure 2.3). Figure 2.4 shows a final production unit with modified structure and conduit wiring. As expected, the modified structure improved system performance and significantly reduced undesired vibration on the supporting structure. Lab and field results of the full system with this modified supporting structure are described in detail in the following section.

2.2 SSL-PZT System Evaluation

The SSL-PZT system that includes all critical parts that influence system performance was assembled and evaluated at the QRDC laboratory, S3i laboratory, CMRL (Coleraine Mineral Research Laboratory) and in the field at Ispat Inland Mining. The solid leg supporting structure minimized interface losses and undesired structure vibration and the system was not sensitive to boundary conditions (installations). Critical parts included a panel, livedeck, split curved resonators, PZT-based smart motors, and a supporting structure. Other parts used that do not influence system performance were: feed box; under-size hopper; and over-size bin. Split curved resonators were used as the final design for two reasons. First, the current magnetic-based production unit uses the same resonators. This makes the retrofitting much simpler. Second, the split resonator was shown to have lower stress levels and therefore, an improved fatigue life.

To optimize system performance, a consistent procedure was adopted every time the system was moved and assembled on a different structure. Calibrations were performed to optimize each smart motor performance for given preloads. For this purpose one motor at a time was turned on and the performance was optimized by adjusting the preload and adding shims between push rod and resonator as necessary. In the final product these adjustments won't be necessary and PZT-based smart motors can be used as plug & play device. The below Figure 2.5 shows the displacement measurement locations on the livedeck for all the tests conducted in the lab and in the field. All data was collected in mils peak-to-peak.

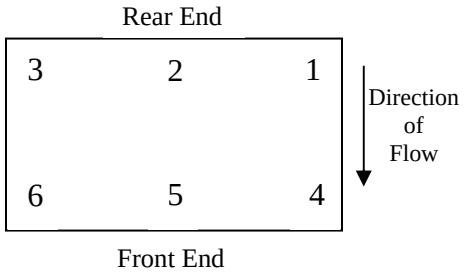

Figure 2.5 Measurement locations on panel

Test results of CMRL and QRDC lab is discussed in detail. However the test results were consistent. Testing at CMRL provided multiple chances to measure the prototype's performance in simulated plant conditions. A comparison of data recorded at two visits to CMRL as well as data collected in the QRDC lab at Chaska show that the SSL-PZT system exceeds the design objectives for panel motion and performs consistently from time to time and place to place. Table 2.2.1 summarizes dry test results recorded on the live deck at QRDC and CMRL. Very little change can be observed, even when moving from a very rigid concrete floor (QRDC) to a relatively soft steel elevated structure (CMRL). Tables 2.2.2 and 2.2.3 compare slurry test results of the SSL-PZT system to the previous prototype design on an absolute and percentage basis. It is clear that the prototype with solid leg frame delivers superior results as compared to the previous prototype. Moreover, the measured levels of stroke meet or exceed existing taconite screening machines powered by magnetic/eccentric mass motor under similar slurry conditions. Finally, noise levels of SSL-PZT system during operation was about 65 dBA, which is below most of the plant background noise by 20 dBA. Noise measurements of the SSL-PZT were not possible during slurry testing at CMRL due to the extreme noise levels created by the pilot plant's pumping equipment. More simply put, the noise generated by the SSL-PZT is lost to plant background noise. This design meets the project requirements and was successfully demonstrated to the DOE and partner companies at CMRL on June 24th, 2005.

Table 2.2.1 Recent Dry Screen Test Results

		QRDC: 3-16-2005		CMRL: 4-11-2005		CMRL: 6-26-2005	
		Frequency 39.7 Hz	Voltage 90 V pk-pk	Frequency 40.4 Hz	Voltage 90 V pk-pk	Frequency 40.5 Hz	Voltage 90 V pk-pk
		Solid Leg PZT System		**Solid Leg PZT System**		**Solid Leg PZT System**	
Point ID		Flow Dir. (mil pk-pk)	Normal Dir. (mil pk-pk)	Flow Dir. (mil pk-pk)	Normal Dir. (mil pk-pk)	Flow Dir. (mil pk-pk)	Normal Dir. (mil pk-pk)
Live Deck	1	32	42	25	41	25	30
	2	33	44	36	45	33	35
	3	27	37	28	38	27	37
	4	31	63	25	64	25	53
	5	32	65	33	63	26	61
	6	25	58	26	54	30	59

Table 2.2.2 Comparison of Slurry Tests

		Ispat Inland: 1-19-2005		CMRL: 4-11-2005	
		Frequency 38.8 Hz	Voltage 193 V pk-pk	Frequency 40.4 Hz	Voltage 193 V pk-pk
		Strap Suspended PZT System		**Solid Leg PZT System**	
Point ID		Flow Dir. (mil pk-pk)	Normal Dir. (mil pk-pk)	Flow Dir. (mil pk-pk)	Normal Dir. (mil pk-pk)
Live Deck	1	10	9	28	36
	2	13	10	32	40
	3	10	9	26	35
	4	9	16	28	58
	5	12	18	34	59
	6	9	17	28	48

Table 2.2.3 Percentage Comparison of Slurry Test Data
(Absolute values can be found in Table 1.2.2)

Point ID		Flow Direction	Normal Direction
Live Deck	1	178%	303%
	2	149%	302%
	3	157%	293%
	4	210%	264%
	5	186%	230%
	6	206%	181%
Average Improvement		**181%**	**262%**

2.3 Smart Motor Longevity Test

The PZT-based smart motor was used for performance evaluation over a period of 2 years. The test article is shown in Figure 2.6. The motor assembly was inserted into the test fixture; the curved resonator was installed between the base block and a 40-lb mass was

attached on the top of the resonator. The entire test article was bolted to the floor. The top mass was equivalent to ¼ of the total weight of a typical live deck. The system was set up with a circular stacked PZT actuator and the system was preloaded. The system was tuned to its first resonant frequency and allowed to run to failure. The driving frequency was set to 12 Hz with an applied voltage of 0-60V (with D.C. offset). The resultant motion was 125 $mils_{pk\text{-}pk}$ in the horizontal direction, measured directly on the resonator tip.

To avoid possible arcing between the ceramic and the surrounding metal parts, the ceramic was first coated with liquid electrical tape and completely covered with black plastic electrical tape. Only the inactive ceramic faces were exposed. Room temperature was maintained between $74\text{-}78^0$F throughout the test.

The test article was set to run round the clock for over two years before failure. The test was started on September 8th, 2003 and failed sometime last week of October 2005. Before disassembling the system, all the electronics, connections, and wires were checked and no problems were observed. On further investigation, it was clear that the ceramic had failed.

2.4 Smart Motor Dynamic Force Measurement

The final test for the smart motors involved a setup that would experimentally determine the output force capacity of each PZT-based device. To accomplish this, the back portion of the smart motor assembly was modified and a PCB Piezotronics force transducer was installed inline with the ceramic (PZT motor). Since only one smart motor assembly was made capable of recording dynamic force using a force transducer, in two separate tests the motor was installed at two locations: one in front and another in the rear. Dynamic forces, generated under operation, were measured under two operating conditions: one motor active at a time, and with all four motors active. Figures 2.7 and 2.8 show the final assembly of this test.

Baseline vibration data was collected on the full system with all four smart motors active. This data was compared with the data collected after replacing one smart motor with a modified smart motor. It was determined that addition of a force transducer did not have any influence on the system frequency or performance. Time trace data showed that force oscillations are smooth sinusoidal wave forms, indicating there is no separation of the push rod from the ceramic/resonator during operation. Below are the details of experimental results:

- Force Transducer Located at Front Right (location 4)
  - Force with front right motor alone – loc. 4 motor active = 475 lbf
  - Force with front left motor alone – loc. 6 motor active = 220 lbf
  - Force with rear right motor alone – loc. 1 motor active = 125 lbf
  - Force with rear left motor alone – loc. 3 motor active = 125 lbf
  - Force with all four motor active = 775 lbf

- Force Transducer Located at Rear Left (location 3)
  - Force with front right motor alone – loc. 4 motor active = 150 lbf

- Force with front left motor alone – loc. 6 motor active = 135 lbf
- Force with rear right motor alone – loc. 1 motor active = 75 lbf
- Force with rear left motor alone – loc. 3 motor active = 450 lbf
- Force with all four motor active = 675 lbf

2.5 Full System Strain Measurement

Strain data was collected on a S3i-101 unit to evaluate the stress levels of critical parts and validate stress results from finite element model. To realize this goal, QRDC approached The Department of Energy (DOE) Albany Research Center (ARC) for strain measurements. QRDC engineers worked with the scientist from ARC to setup the system. This task was successfully completed. This report briefly summarizes the process taken to measure and record strain data, ODS and stroke/acceleration data, as well as the process of correlating that data to the FEA model.

2.5.1 Strain Measurements

The strain gages used in this investigation were foil-type gages. These gages are created by bonding a very thin metal wire to a flexible substrate. This flexible substrate can be bonded to the surface of a test object. As the structure changes shape, the wire is stretched or compressed, changing the wire's resistance. Figure 2.9 shows the side view of S3i-101 unit with strain gages.

2.5.2 ODS and Stroke/Acceleration Measurement

The purpose of measuring ODS and Stroke/Acceleration data is to ensure that the operating shape of the machine is known and the actual displacement during operation can accurately be matched by the FEA model. This is an effective means of ensuring the validity of comparing stresses in the tested machine to stresses in the model.

2.5.3 ODS and Stroke Correlation

The first step in comparing the results of the ODS and stroke measurements was to calibrate the FE model. This was done by varying the excitation level of the FE model until the predicted output at a selected point on the structure matched the experimentally measured response at that location. For all data points with substantial motion on the livedeck, the FEA data matched the test data within 15% in both vertical and horizontal directions. Figure 2.10 shows an experimental and FEA stroke comparison graph.

2.5.4 Stress Measurement Correlation

In order to compare the experimentally measured strain data and FE stress data, post-processing of the strain data was necessary. Matlab® software was used to post-process time domain strain data and convert it to Von Mises stress. For proper correlation of FE and test data, only steady-state data was taken into consideration throughout the analysis. Figure 2.11 shows a typical time trace data on the resonator.

Equation (1) was used to transform the individual strain signals into the complementary principle stress time histories. These results were used to calculate Von Mises stress using equation (2).

$$\sigma_{1,2} = \frac{E}{2(1-\upsilon)}(\varepsilon_A + \varepsilon_C) \pm \left[\frac{1}{2(1+\upsilon)}\right] \cdot \sqrt{(\varepsilon_A - \varepsilon_C)^2 + (2 \cdot \varepsilon_B - \varepsilon_A - \varepsilon_C)^2} \quad (1)$$

$$\sigma_V = \sqrt{\frac{(\sigma_1 - \sigma_2)^2 + (\sigma_2 - \sigma_3)^2 + (\sigma_1 - \sigma_3)^2}{2}} \quad (2)$$

Figure 2.12 compares stress results of finite element model with that of experimental results. The graph shows a nearly identical trend in the stress data; however FE results tend to be higher. This make sense and was expected as the current FE model considers perfect conditions and does not take into consideration any losses at the various interface, which makes the system stiffer than the real world condition.

2.6 Production Unit Requirement

The SSL-PZT system was tested successfully at CMRL and meets the project performance goals in terms of vibration and metallurgical results. The system, however, needs few refinements before production of this innovative system can be realized. What follows in this report is a brief description of areas of improvement and possible solutions.

2.6.1 PZT/Smart-motor Design and Packaging

QRDC does not currently have a robust, reliable, production ready smart motor. Even though the longevity test of smart motor, using quarter system under laboratory conditions, was successful, motor failures were encountered during field testing. Currently, the system operates at its maximum capacity. More powerful motors are needed to provide additional capacity in instances where plant conditions require more power.

Furthermore, Smart-motors need to be packaged to survive in harsh environments. In the current design, a seal is in place but is not robust enough to avoid moisture buildup inside the packaging during prolonged exposure.

2.6.2 Electronic Equipment

Equipments (amplifier, function generator etc) used were laboratory grade and most of them are not suitable for industrial use. Sources for production grade instruments need to be identified and business relationships developed.

2.6.3 Production Ready Control Scheme

QRDC does not have packaged control hardware to continuously monitor SSL-PZT performance and tune automatically subject to change in operating conditions. As with the other electronics, suppliers will be identified and the hardware sourced.

2.6.4 Structural Refinement

Frame redesign is necessary to better incorporate coil spring suspension for performance as well as structural stability. The frame should be redesigned so that the springs are recessed into the machine legs. In the current configuration, the springs may

slowly become packed with taconite, making them less effective over time. Installation of feed box and undersize hopper should be reviewed to account for changes in frame height created by the coil springs.

CHAPTER III – DRY APPLICATION DESIGN & ANALYSIS

The Department of Energy (DOE) awarded one year contract extension to QRDC Inc. to investigate feasibility of using SmartScreen™ technology in dry screening application. During that time, a commercial partner was identified in food processing industry and their seed cleaning system was examined. This chapter examines a number of design opportunities for this seed cleaner, and illustrates how they were addressed in the most recent design of a laboratory seed cleaner prototype.

3.1 Overall Seed Cleaner Design

During the first quarter, the QRDC team (with the help of S3i team) identified a product and application to initiate a feasibility study. To realize the goal, a laboratory sized grain cleaning and separation machine. Details regarding this partner are deferred to Appendix A in respect of the partner's identity. What follows in this session is brief description of the machine, vibration measurements and design opportunities to insert SmartScreen™ technology identified by QRDC.

3.1.1 Machine Description

This machine is used in the food processing industry for grain cleaning and separation. The machine consists of six primary components:

- Machine Frame
- Shoe
- Screen Panels
- Shoe Actuation System
- Feeding System
- Air Handing System

The machine frame refers to the steel superstructure of the seed cleaner. The shoe is moving part of the machine which houses the screen panels. The shoe is constructed of a special type of plywood made to be moisture and insect resistant. It is suspended from the machine frame by four steel straps and has a pendulum like motion. Three screen panels can be placed in the shoe. Material flow is directed so that material passes over each screen in series. In wheat processing (the primary concern during this investigation) the top deck is used to remove large oversized particles. The second and third decks are used for near size separation. The shoe is actuated by motor and mechanical linkage consisting of a belt and pulley for speed reduction, eccentric masses, and a connecting rod. The speed of this is variable on the laboratory unit, but is often fixed in industrial applications. Material feed into the machine is controlled in two ways. A metering roller is motor driven, allowing for the speed to be changed. Also, the gap between the hopper and metering roll is variable. The air handling system is the most complex part of the design. It is used to pull light and fine particles out of the material flow. This is done at many places throughout the machine and is controlled by five independent controls.

3.1.2 Vibration Measurement

The objectives of this task were: (1) to gather baseline vibration data for purpose of system dynamics characterization, (2) to outline recommendations for a proposal based on vibration results. Modal data and operating deflection shapes (ODS) were extracted on each individual panel and the shoe. Figure 3.1 shows a typical frequency response function of the shoe. In case of shoe modal analysis, two cases were considered, first with the rigid link between the eccentric motor and shoe in place and then with the link removed, allowing the shoe to move freely on the supports. Figures 3.2 and 3.3 show the FRFs of these two cases. From ODS measurements it was observed that the motion of the shoe is dominated by the front-to-back direction (flow) and very little vertical motion is observed.

Stroke data was collected on multiple points of the 16 round top panel screen, 5 slot bottom panel screens, and shoe using the same measurement points used for modal and ODS data collection. Average results for individual components and the system as a whole are presented in Table 3.1.1.

Table 3.1.1 - Stroke data for Seed Cleaner

Component	Side-to-Side [mil pp]	Front-to-Back [mil pp]	Vertical [mil pp]
5 Slot Bottom	42	1161	145
16 Round Top	87	1179	138
Shoe Right	24	1160	40
Shoe Left	43	1176	30
System [All pts avg]	49	1169	88

3.1.3 Design Opportunities for QRDC

After gaining working knowledge of the machine and detailed vibration measurements, the project team identified several opportunities where QRDC technologies could be applied to improve machine characteristics. Two main areas are discussed in the following sections.

Shoe Actuation System: Currently, the unit employs a 370 W single phase AC motor to drive the shoe. The mechanical linkage between the shoe and the motor's output shaft is fairly complex, involving a connecting rod, a secondary shaft with eccentric masses, and finally a belt driven pulley.

The first priority in implementing SmartScreen™ philosophy was to remove the eccentric mass drive system. Due to the large stroke requirements, it seems that the application is better suited for a magnetic drive system, than a PZT based actuation of the overall shoe. Even with a large stroke actuation system, a mechanical amplification will be needed to obtain the machine's current stroke levels.

Screen Actuation System: Random impacts by many rubber balls are used to excite the screen surface, thereby preventing screen blinding. Without this, the 5/64 slotted screen became almost completely blinded during operation. The rubber balls, each approximately 10gr mass and 25mm diameter, rest between ridges in the tray. During operation, the balls

bounce randomly around between the ridges and screen surface, knocking trapped particles out of the screen holes. Even with this system, some screen blinding has been observed.

It was identified that PZT actuators could be used to excite the screen surfaces. The advantages of this are numerous. First, the inertia of the shoe will be reduced by removal of the mass of the ball decks. This will reduce energy consumption and ultimately reduce energy transfer to the surrounding environment. Second, the shoe design can be simplified. Finally, PZT based screen actuation can allow for the screen input to be tailored, maintaining the deblinding characteristics while reducing the noise created by the ball impacts. Testing at QRDC revealed that the average operating sound pressure level (SPL) dropped by about 8 dB by simply removing the balls.

3.2 Overall Smart Seed Cleaner Design

The overall design of the Smart Seed Cleaner designed by QRDC is shown in Figure A.4.2. This design incorporates a single-source drive approach, a novel system tuning device, a simple and compact solid frame, and the same shoe design that is currently used by QRDC's commercial partner. An additional part of the design is a novel deblinding approach, which utilizes PZT patch in combination with coil-springs and costs very little in terms of added mass.

3.2.1 Single Actuation Energy Source

An electromagnet actuation method has been chosen to both move the shoe and activate a deblinding mechanism based on a coil-spring/mass system. As the shoe moves due to the forces imparted on it by the electromagnet, masses suspended by coil springs are energized enough to impact the individual screens. The design of this drive system is illustrated in Figure 3.4.

A few key design concepts for the electromagnetic drive system should be noted. First, a drive of this kind prevents the need for any mechanical linkages between the shoe and the driving mechanism. This allows for the possibility of a drive failure or replacement without necessarily halting the system operation (for example, if another drive was still active). Secondly, the design developed incorporates a shimming technique that enables the user to easily move the magnet closer to and farther from the shoe without requiring addition or subtraction of material, as in the traditional approach to shimming. This same feature allows for the magnet to be set at an angle to the vertical, as would be helpful when more displacement is expected at one point than another (see Figure 3.5). Additionally, the current design allows for movement of the magnet in a vertical direction. This is accomplished through a loop hole pattern on the units frame that attaches to the back-plate of the drive with bolts. Finally, the drive's adapter plate is suited for either a larger electromagnet or a smaller one, simply by using different hole patterns. These hole patterns could, of course, be customized to the hole pattern of any magnets that fit within the footprint of the adapter plate.

3.2.2 System Tuning Approach

The primary principle that allows this machine to work at such large energy savings is resonance. Resonance frequency is based on the stiffness of the system as well as its weight.

Since the weight of the shoe and its contents may change based on application, the stiffness should be alterable in case a relatively similar frequency would like to be maintained. Additionally, there may be times when a higher or lower frequency may want to be targeted. Therefore, a simple tuner was designed to allow for changes in the resonator effective length, which will change the stiffness of the system respectively. Figure 3.6 illustrates the concept. Analyses indicate that this simple mechanism can offer a frequency change span of 2-3 Hz.

3.2.3 The Frame

Figure 3.7 illustrates the frame design for this system. It is intended to be compact, rugged, simple, and functional. The cross-section of the steel piping is 2" x 2" x 1/8", with gussets used where needed. The back end of the frame is left open for access to the back of the shoe, as is the top of the frame. Mounting pads with appropriately tapped holes are welded where the resonators are to be held. Additionally, the plates required for the magnetic drive system installation are included as a permanent weldment.

3.2.4 The Shoe

Figure A.4.3 illustrates the shoe design. This is the same design that was explained in section 3.1 and also introduced in the last semi-annual report. This design is very similar to that used by an industry leader in seed separation.

3.2.5 A New Approach to Deblinding

Blinding is a constant problem in the seed cleaning industry, due to the tight tolerances required for the products. A number of approaches to deblinding of screens have been in use for years, but most add significant weight, complexity, or required energy to the system. QRDC has recently been working on new concepts that should minimize all three of these setbacks. These approaches can be separated into two groups: 1) components that provide a passive, impulsive excitation of the screen panel with mechanical components, and 2) direct excitation of the screen panel with active PZT-based components. Figures A.5.1 and A.5.2 depict the basic principles and components.

CHAPTER IV – DRY APPLICATION TESTING & RESULTS

Fabrication of the dry-application cleaner was completed during this contract period, with very promising preliminary results. Figure A.6.1 shows a photograph of the system taken at QRDC's facility. A feeding mechanism to help dispense the seed at a 600-700 lb/hr rate was also added during this reporting period. The seed used for testing was wheat.

4.1 Frequency Calibration

The first verification after assembly was completed was of the operating frequency (natural frequency) of the system with and without seed. It was found that with the resonator tuners placed in their lowest position (highest frequency) the natural frequency without seed is about 5.25Hz. When incorporating the seed at 600-700 lb/hr, the added weight brings the frequency down to 5.15Hz. This agrees very well with analytical models of the system, which predicted frequencies between 5 and 7 Hz. Lower frequencies can be reached if the resonator tuners are adjusted appropriately. It should be noted that the fastening torque used is very significant in the operating frequency outcome.

4.2 Horizontal Stroke Achievements

Once the frequency of the system was verified, it was necessary to discover whether the required stroke of $1"_{pk\text{-}pk}$ could be readily achieved. It was found that, even with the 600 lb/hr seed flow, as much as $1.25"_{pk\text{-}pk}$ horizontal displacement could be realized with very little power draw by the magnetic motor controller.

Rotation of the shoe has also been checked by monitoring the horizontal displacement at two corners of the shoe. Based on these results, it is safe to say that any rotation (if it exists) is very minor, and was certainly not detected with the displacement sensors (LVDTs) used for our testing.

4.3 Power Measurements

As was mentioned above, the power required to keep the system running was very low. Energy consumption calculations of this unit when compared to production unit showed over 60% reduction. Under operation while processing seed, Smart Seed Cleaner consumed 200 watts compare to 550 watts consumed by production unit. This resulted in an energy savings of about 64%. An added benefit, Smart Seed cleaner is that the system is fully operational with only one electromagnet. That is to say that, if one of the two magnets were to stop operating, the other could keep the unit running at the same 1" stroke, at the same frequency, and with a similar power draw. This is a significant improvement over the current systems in the field that operate with a linked rotary system that must be halted and kept off-line in the event of a motor failure.

4.4 Deblinding Results

The deblinding test results have been very promising. The combination of two deblinding mechanisms has resulted in over 90% deblinding of the screen when compared to no deblinding apparatus. Preliminary results for this approach have been collected, based on a lab-fabricated prototype. So far numerous locations for the patch and spring-ball have shown promise, and numerous seeds such as wheat, lima beans, and soy beans, have been successfully processed with minimal blinding. Further testing and modifications may lead to an approach that works even better than the current ball-deck strategy unit or other commercial suppliers. It should be noted that all results are still preliminary and subject to further, more thorough testing. Table 4.1 compares QRDC designed Smart seed cleaner performance and specifications with that of the commercial unit.

Table 4.1 comparison between Smart seed cleaner and production unit.

	QRDC/S3i Smart Seed Cleaner	**Production Unit**
Operating Speed	300-360 RPM (5-6 Hz)	240-300 RPM (4-5 Hz)
Range of Operating Speed	TBD	Fixed
Horizontal Stroke	1.25 $in_{pk\text{-}pk}$	1.25 $in_{pk\text{-}pk}$
Stroke Range	0 to 1.5 $in_{pk\text{-}pk}$	Fixed @ 1.25 $in_{pk\text{-}pk}$
Supported Seed Flow Rate	600 lbs/hr	600 lbs/hr
Drive System	1 Electromagnet	Eccentric Drive & Linkage
Optional Drive System	Redundant Magnet	None
Power Draw for Gross Shoe Motion w/ Seed	200 Watts	550 Watts
Blinding Prevention Mechanism	Dual Component Mechanism	Ball Deck
Weight of Blinding Prevention Mechanism (per deck)	1 lb	11 lbs

CHAPTER V - ENERGY SAVINGS & ECONOMICAL BENEFITS

One of the key benefits of the Smart Screening System (S3) is significant energy savings. The state-of-the-art Smart Screening technology uses miniaturized motors, based on smart materials, to generate the shaking. The underlying technology is based on QRDC's Energy Flow Control™ (EFC™), Vibration Control by Confinement™ (VCC™) , and Smart ScreensTM. These concepts are used to control, confine, focus and intelligently manage the energy flow for efficient and effective screening. The functional demonstrated S3 unit uses four PZT based Smart Motors and requires 90% less energy when compared to the conventional screening machines and also addresses problems related to noise and vibration, screening efficiency, productivity, maintenance cost, and worker health.

Conventional screening machines use decades-old technology that relies on brute force to generate shaking. This brute force is generated through rotary electrical motors with eccentric rotor that provides periodic forcing function. These vibration-based screens use bulky motors, generate excessive uncontrolled shaking, and waste significant energy in undesired structure motion/deformation. Examples of currently marketed products are shown in Figure 5.1. High noise levels, undesired vibrations, excessive energy consumption and maintenance cost, and low efficiency are among the disadvantages of these systems. Limits to control of vibratory energy flow and screen blinding (plugging of screen openings) are the main causes of lower performance and throughput. In most cases, frequent checks are required and screens have to be cleaned manually using water jets, mechanical devices or with manual tools, thus further increasing the energy consumption. Overall, the current screening machines are energy intensive and have very low performance to cost ratio.

An energy survey conducted at Minntac (US Steel) revealed that inefficient screening contributes towards process energy loss. Even though screening and size separations are not the single most energy intensive process in the mining industry, they are often the major process bottleneck. The Minntac plant has 114 fine wet screens and 45 rock dry screens. The moving parts (live deck) of each screen weights 850 lbs to 1100 lbs, or a total of more than 135,150 lbs. The plant currently uses approximately 200 megawatts of electrical power daily and current screening technology (114 units) consumes over 1.5 megawatt hours of electrical energy each year. Poor screen recovery (screen blinding) increases the re-circulating load of the line. This in turn reduces the rod mill feed by at least 20 tons per hours or 5% of the line capacity. **Poor screening recovery contributes to lost or wasted energy, estimated at 2,494 megawatts hours each year at Minntac plant alone.** Also assessment of noise and vibration data in the vicinity of these screens showed noise levels as high as 107 dBA and high vibration levels. Similar machines are often used in O&G industry, food processing and other dewatering and mixing industries.

Given the current energy scarcity and ever increasing demand, it is highly desirable to improve the technologies used in screening industry including dewatering application. Innovation in vibration generating technologies has made it possible to create vibration in wide range of consumer products ranging from massage chairs, to cell phones, and even tooth brushes. These products do not use unbalanced rotating mass to generate shaking; rather they use smart materials combined with optimized mechanical components. The

developed Smart Screening System is also based on similar state-of-the-art technologies and addresses the shortcomings of conventional screening machineries discussed above.

As shown in Figure 5.2, S3 uses miniaturized motors that can be hand carry compare to convention motors that require a crane and two or more workers are needed for transport and installation. Due to improved controllability, S3 focuses its energy to the sieves (screen panel) (refer to Figure 3). In other words S3 does not shake the entire unit or the supporting structure or surroundings.

The above concepts and discussion have been validated through the successful development and demonstration of Smart Screen System. This system uses a PZT-based Smart Motor to generate shaking along with mechanical motion amplifiers. The table below provides the anticipated energy savings through S3 technology.

Table 1 Energy benefits, assuming $0.05 per kW-hr cost and constant iron ore production

Electric Energy Source	**Relation**	**Quantity**
Current Technology Usage	A	2.3E6 (BTU/Ton)[1]
Proposed Technology Usage	B	5.75E5 (BTU/Ton)[2]
Electrical Energy Savings	C = A - B	1.73E6 (BTU/Ton)
Iron Ore Production 10 years[3]	D	1.50E8 Ton
Cumulative Energy Savings	E = C x D	2.59E14 (BTU/10 Yr)
Cumulative Savings	F = (E / 10,5000) x 0.05	**$1.23E9 over 10 Yr**[4]

[1] Industry average
[2] Based on minimum anticipated 75% reduction in energy requirements (96% reduction in laboratory with S3)
[3] MINNTAC production
[4] Power generation rate is 10,500 Btu/KW, energy cost at $0.05/KWHr

Based on information provided by MINNTAC, the current energy use at MINNTAC is estimated at $85 million per year. The daily operation cost is estimated at $1 million. MINNTAC and Inland Mining produce 15 million tons and 2.65 million tons of iron ore annually, respectively. These two productions add up to be about 31% of the total domestic production (57 million tons). The seven ore operations in Northern Minnesota produce 43 million tons, 75% of the total domestic production. MINNTAC and Inland Mining, our mining partners, are convinced that our proposed approach is the first step in making their processing operations more competitive in the global market.

Other economical benefits include 1) environmental benefits through reduce energy consumption, reduce weight (or less material) and elimination of lubricants and other various components. 2) Improve worker health and safety through reduce noise and vibrations, and less distraction by eliminating ear protection for noise.

In summing up the achievements of QRDC team during the DOE funded project, the team has successfully demonstrated the proposed energy and economical benefits. These benefits include, over 90% decrease in energy requirement to operate the screening machinery, increase safety through noise and undesired vibration reduction, improved productivity through better control on the energy flow, larger screening area and capabilities to minimize screen blinding.

CHAPTER VI – CONCLUSION

In this report, our progress and achievements during the course of this DOE funded project is detailed. It was shown that the program has been very successful and all tasks has been completed or exceeded the requirement. The implementation of Smart Screen technology in various applications such as mining and food processing industry has shown very promising results and potential to save significant energy.

Initial assessment on vibrating fine screens at a taconite ore processing plant and food processing lab unit was completed. Based on the assessment results, it is clear that the current screening machines need improvements to effectively and efficiently process screening material. Current screening machines not only generate loud noise and transmit vibration to the surrounding structures but waste lot of energy due to undesired structure deformation and old technology. Two main areas that need to be addressed were identified in the current screening technology. These areas are:

Shaking mechanism: Bulky electrical motors with bearings and rotating unbalance mass generates shaking. These moving parts are the main source of excessive noise and vibration, heat and higher maintenance costs. Our smart motors can replace the conventional, inefficient motors, and have been shown in the field to reduce weight by 80%, and energy by 50-95%. Sound levels consequently have been brought down dramatically, so that the machine noise is below the plant background noise and no longer detrimental to worker health and safety. In terms of screen acceleration levels and displacements, Smart Screens have proven to meet and exceed vibration levels in the field while dramatically cutting down on the vibrations transmitted to other structures. For the dry screening application, QRDC has shown that smart alterations to the system can reduce the energy consumption from 525 Watts to less than 200 Watts.

Technology limitation: Current screens have limited flexibility on frequency of shaking, type of shaking, orientation of shaking, and magnitude of input force. These factors affect the material separation process and lead to screen blinding. The Smart Screen approach continues to address these issues through innovative ideas such as the use of PZT materials for dry screening application. It has been demonstrated through experimentation that blinding prevention mechanism (BPM) can do similar or better job than the existing mechanisms while eliminating complex mechanisms and significantly reducing the weight requirement.

SmartScreens™ technology offers solutions to the above problems. Through this technology, the energy flow and the motion of the screen are controlled more efficiently and effectively. Use of miniaturized motors offered greater flexibility to control speed of operation, type of motion and its magnitude, and noise free operation. S3 eliminates and/or downsized many of the structural components. As a result, the surface area of the screen increased for a given space envelope.

During this project, conceptual resonator designs were developed for the proposed SmartScreens™, along with a new actuating mechanism and a new supporting structure. The

resonators, motors, and supporting structure were analyzed and tested for performance, and based on the results, were down selected and incorporated in the full system. Completion of this taconite system led DOE to grant QRDC an additional award for the purposes of evaluating the feasibility of Smart Screen technology in the dry application industry. Thus, a commercially viable seed-cleaning system was introduced and tested, proving the promise of the SmartScreens™ application in multiple industries.

FIGURES

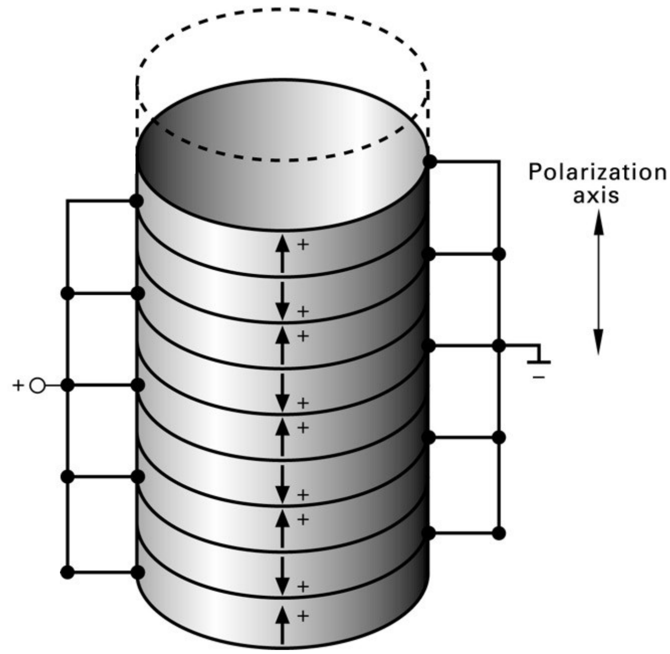

Figure 1.1 Diagram of circular PZT stack

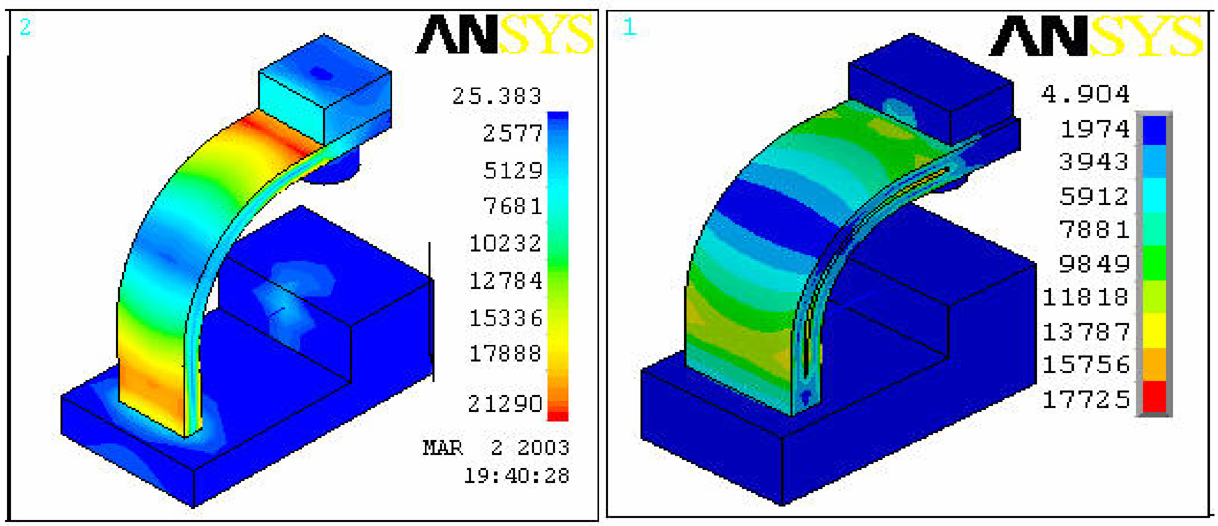

Figure 1.2 Stress distribution on resonator; single resonator (left) split resonator (right)

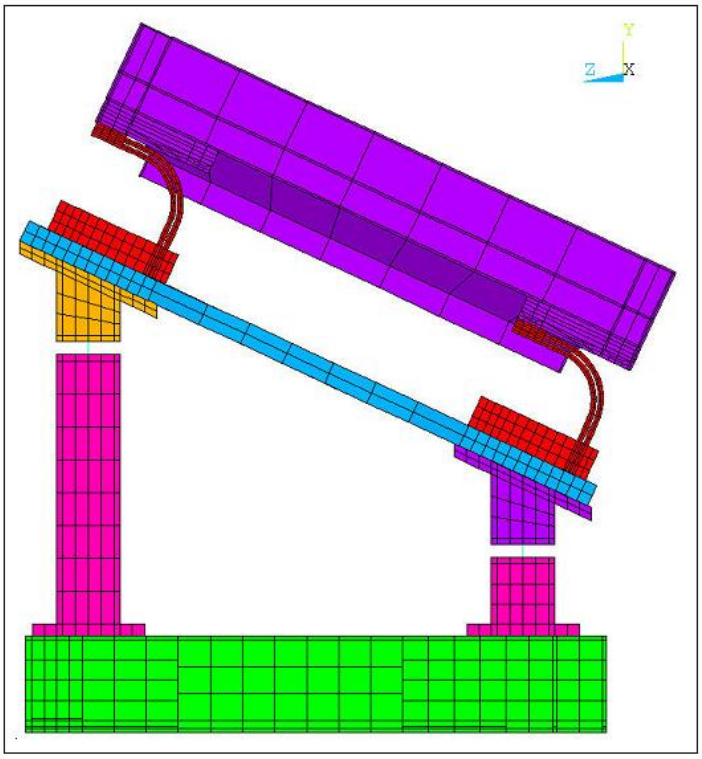

Figure 1.3 Model of suspended production unit

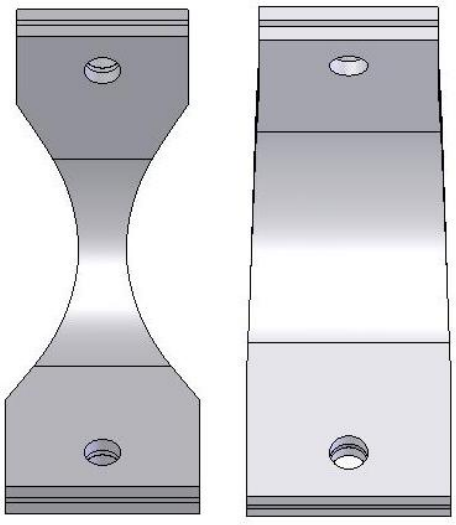

Figure 1.4 Resonator tapered along width (2 extreme cases)

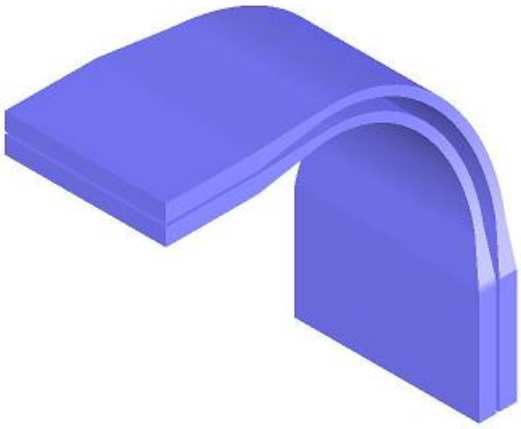

Figure 1.5 Resonator tapered along thickness

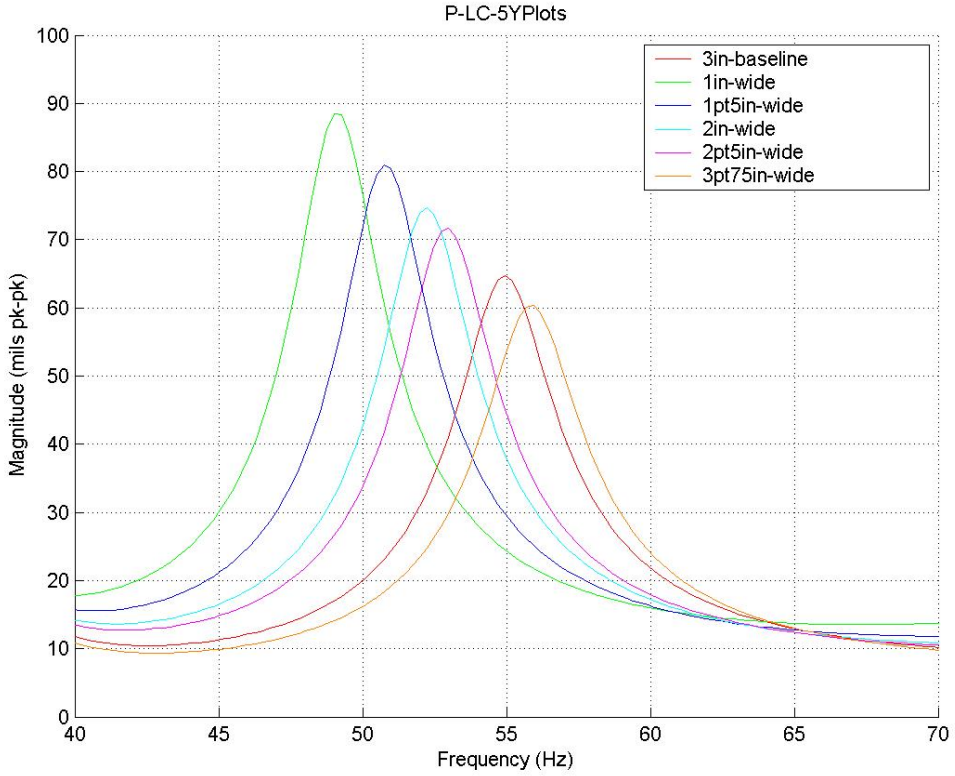

Figure 1.6 Case1 – vertical displacement comparison at front (discharge) end center

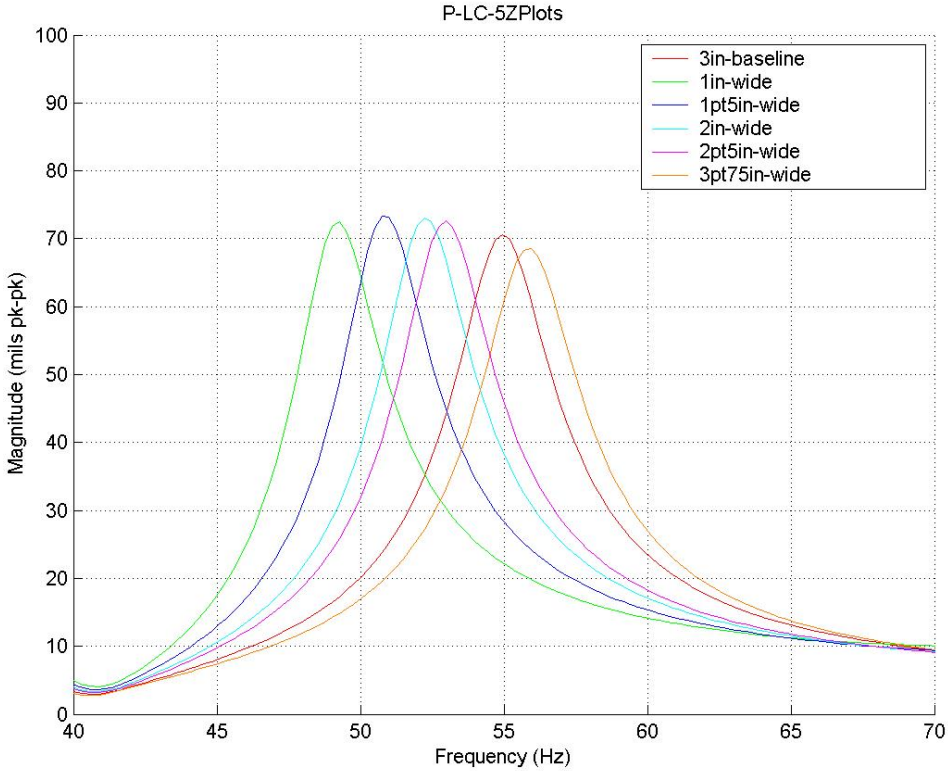

Figure 1.7 Case1 – horizontal displacement comparison at front (discharge) end center

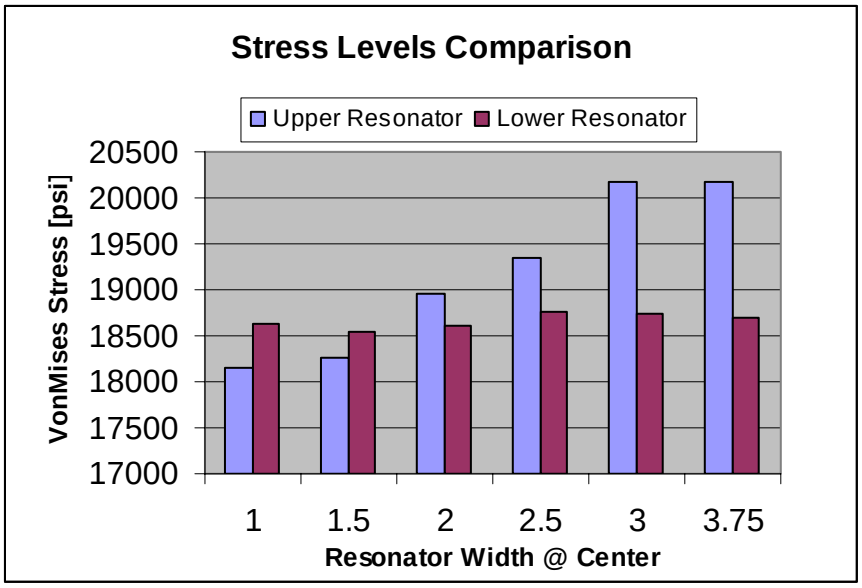

Figure 1.8 Case1 – Stress levels comparison with varying resonator width

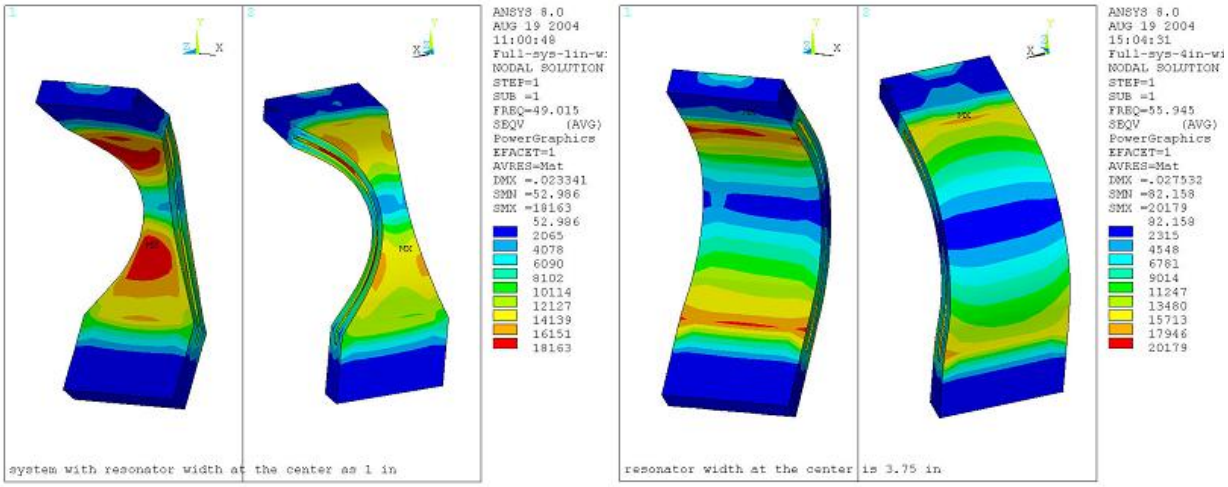

Figure 1.9 Case1 – stress levels & distribution on resonator for extreme cases

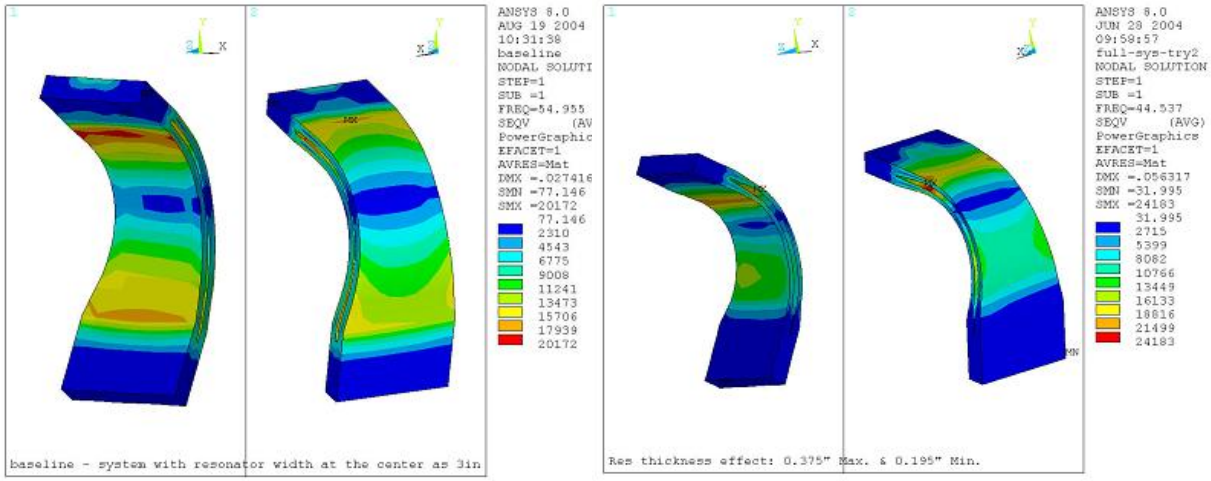

Figure 1.10 Case2 – stress levels & distribution on resonator; Left: baseline; Right: Case 2

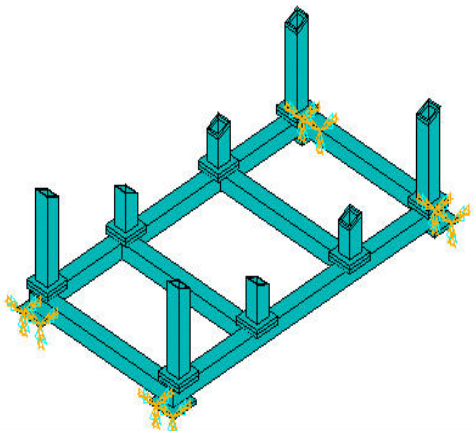

Figure 1.11 – Tubular Supporting Structure Design

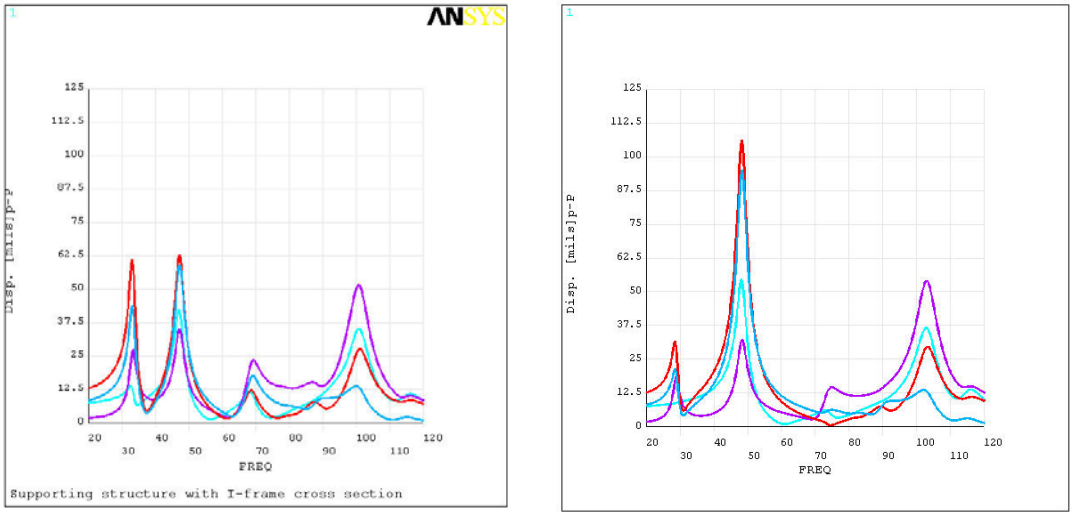

Figure 1.12 Live deck displacements for I-frame structure (left) versus tubular structure (right)

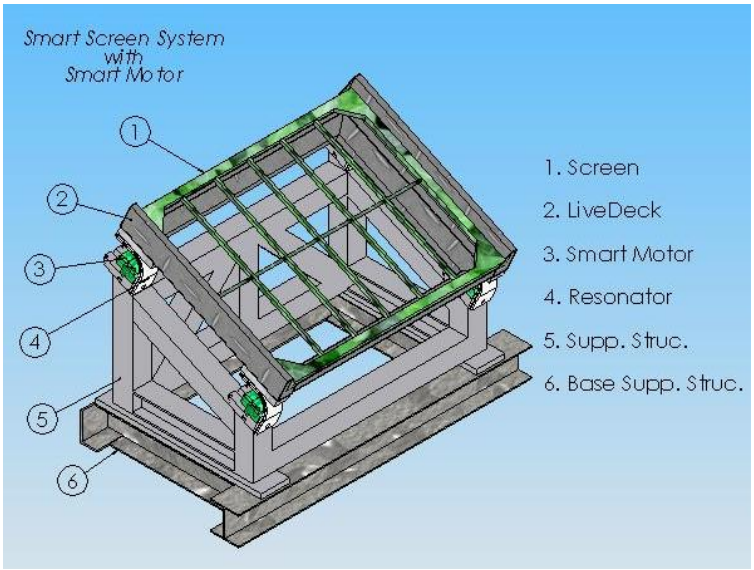

Figure 1.13 Supporting structure design without static

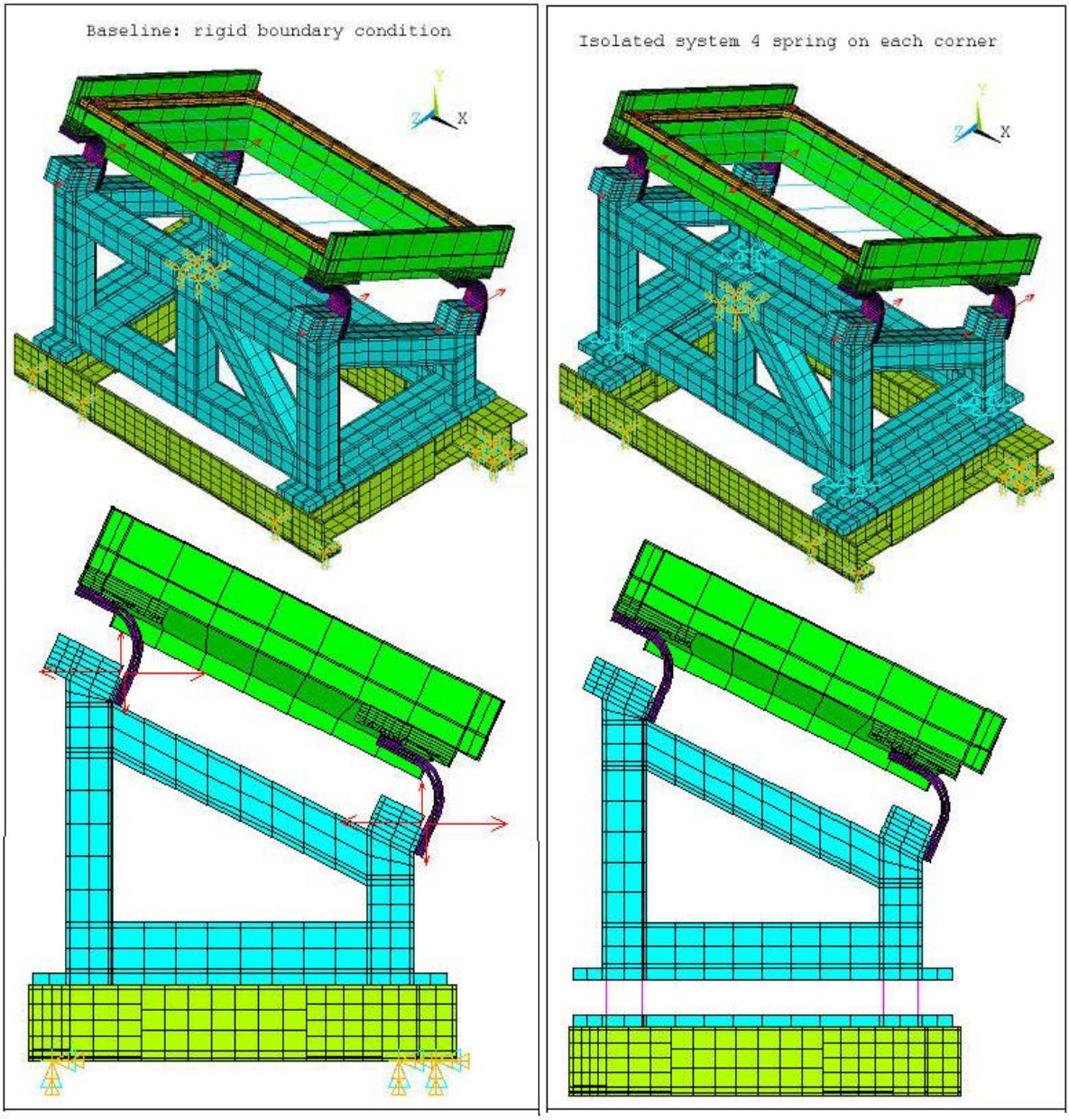

Figure 1.14 PZT system isolation study; Left: fixed system; Right: suspended system

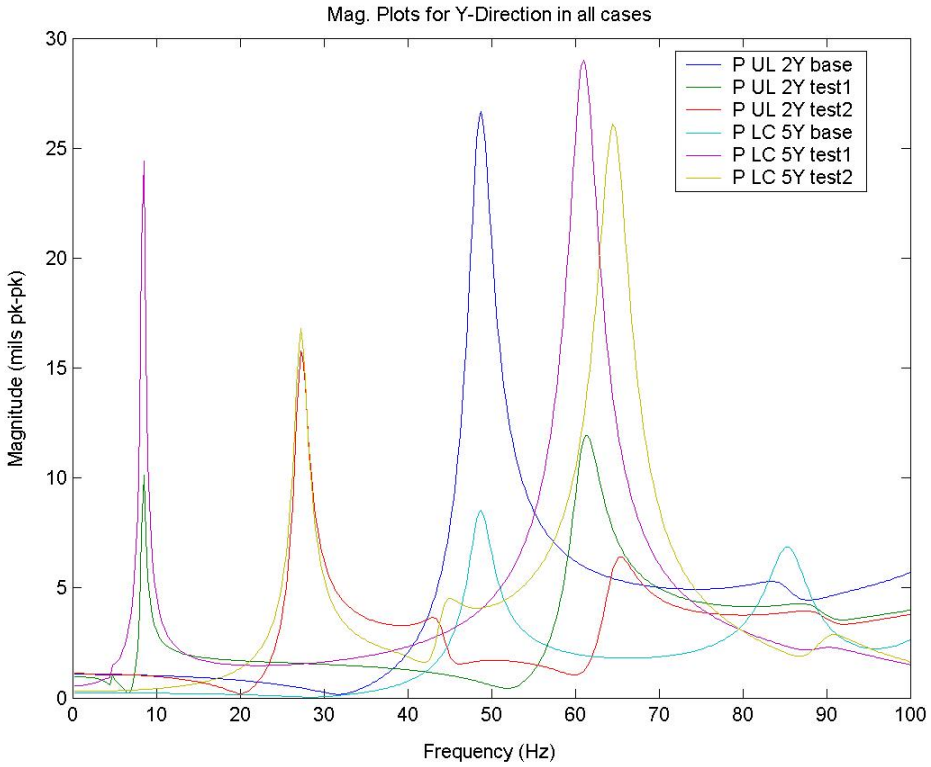

Figure 1.15 Displacement comparisons at rear & front end in vertical direction

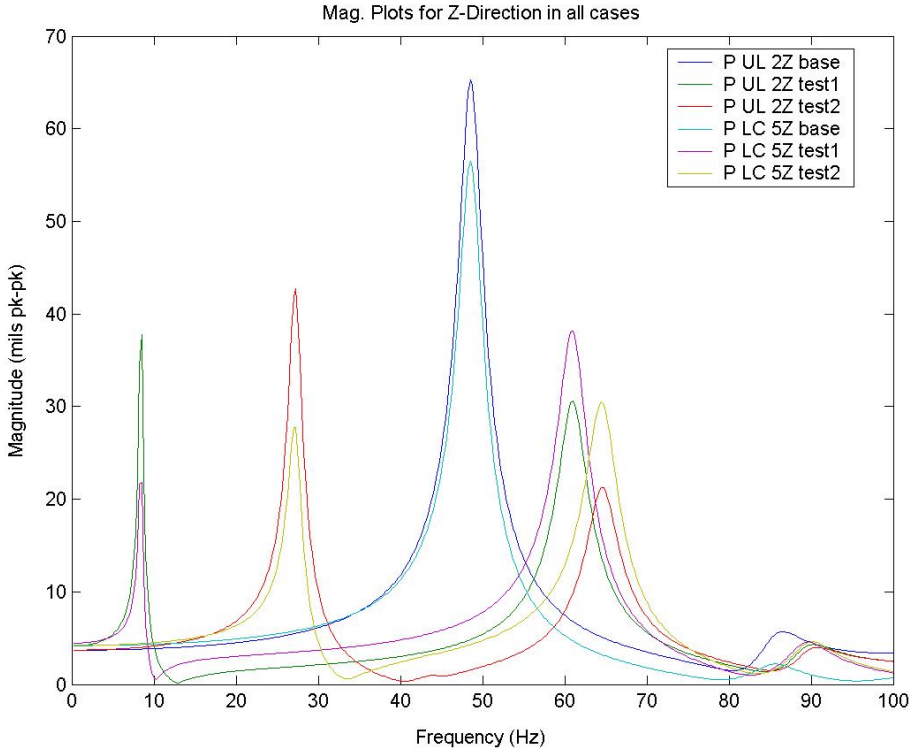

Figure 1.16 Displacement comparisons at rear & front end in horizontal

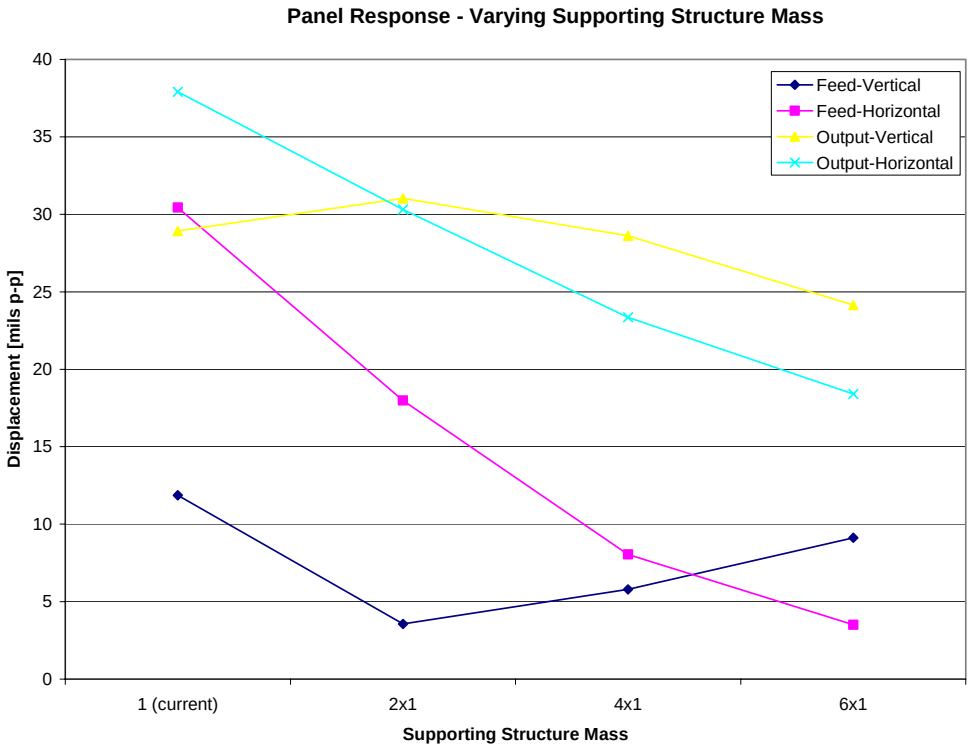

Figure 1.17 Panel response with varying supporting structure mass

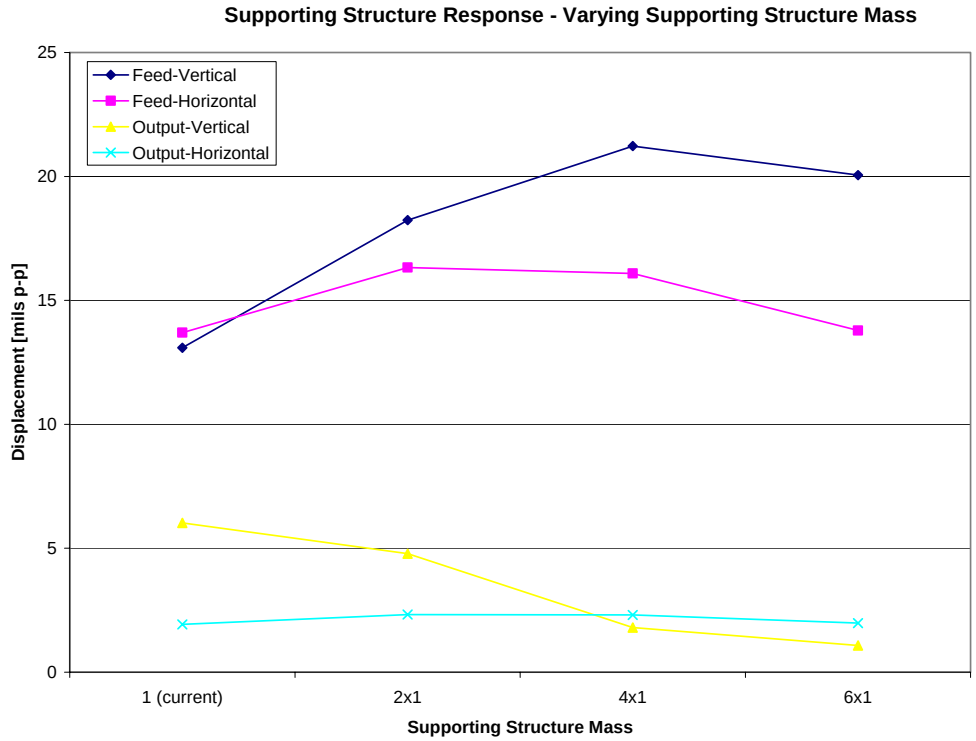

Figure 1.18 Panel response with varying supporting structure mass

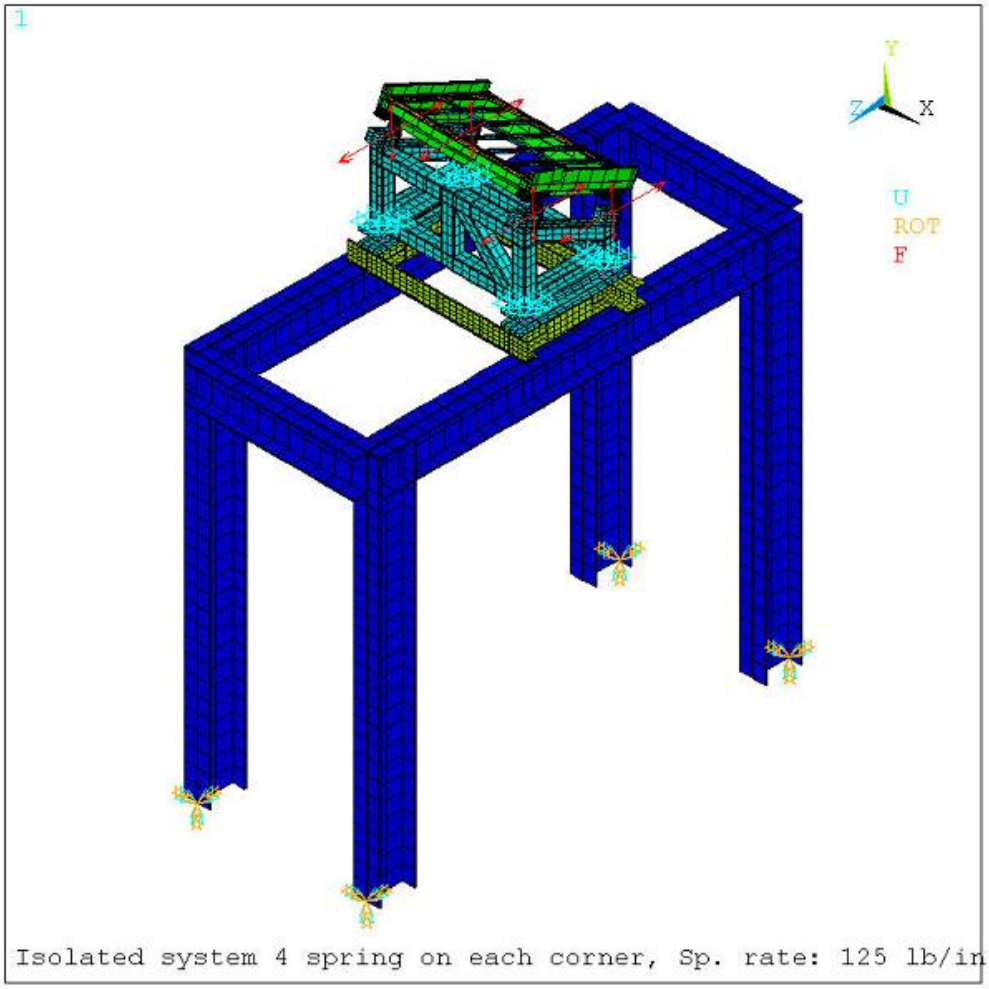

Figure 1.19 I-Cross section beam structure simulating plant structure

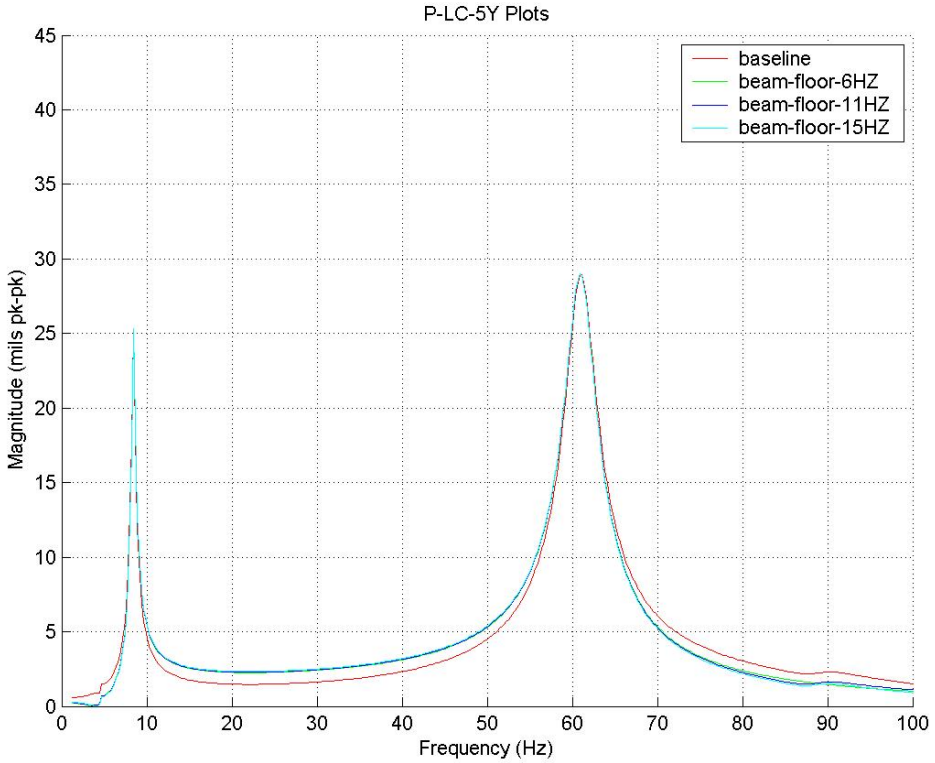

Figure 1.20 System response at front end in vertical direction with varying plant structure

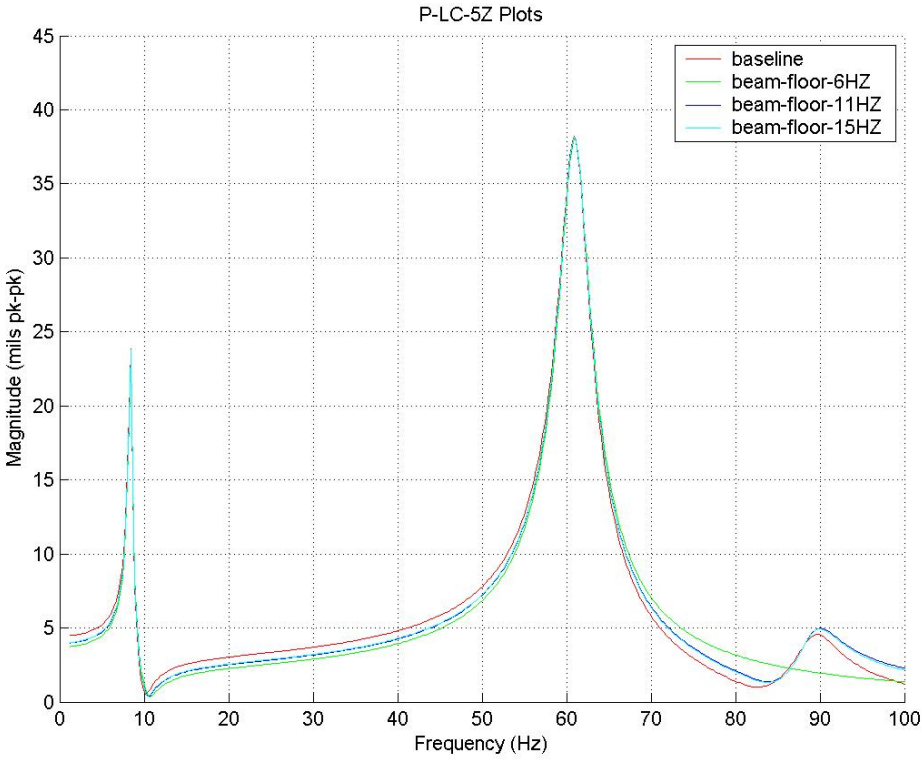

Figure 1.21 System response at front end in horizontal direction with varying plant structure

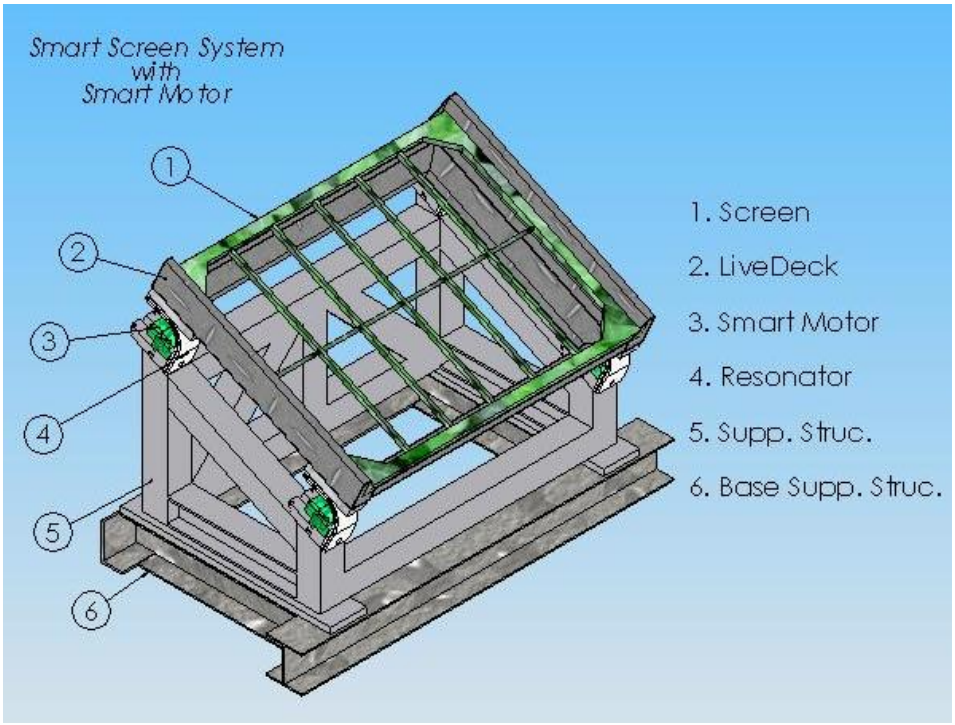

Figure 2.1 Model of SmartScreen™ system with modified supporting structure

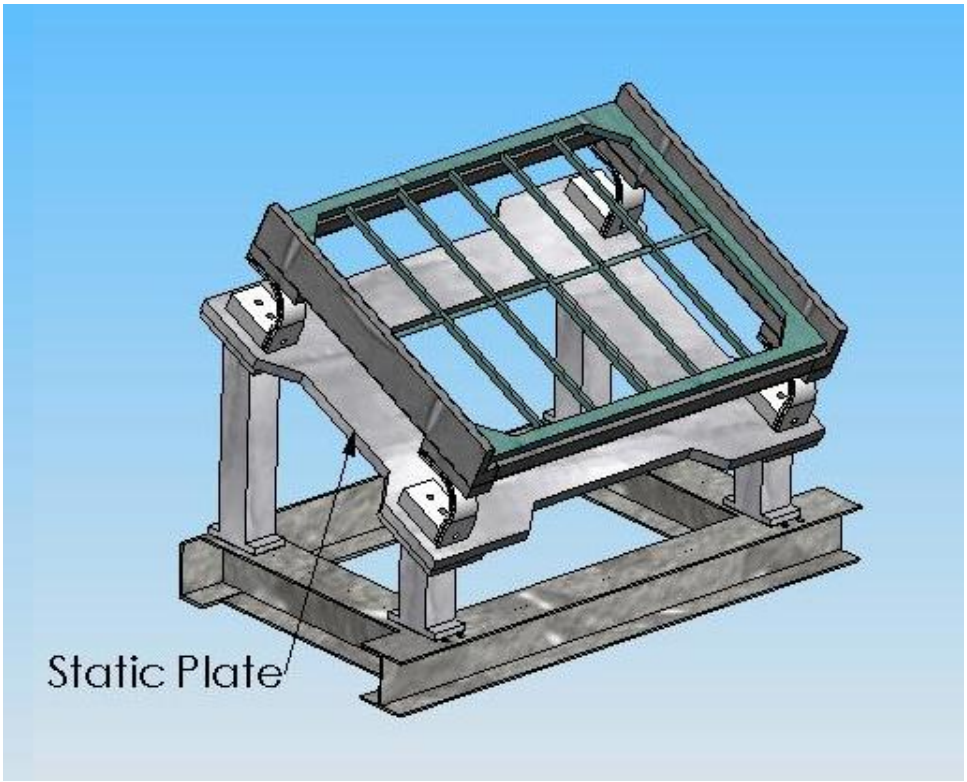

Figure 2.2 Model of SmartScreen™ system with old supporting structure

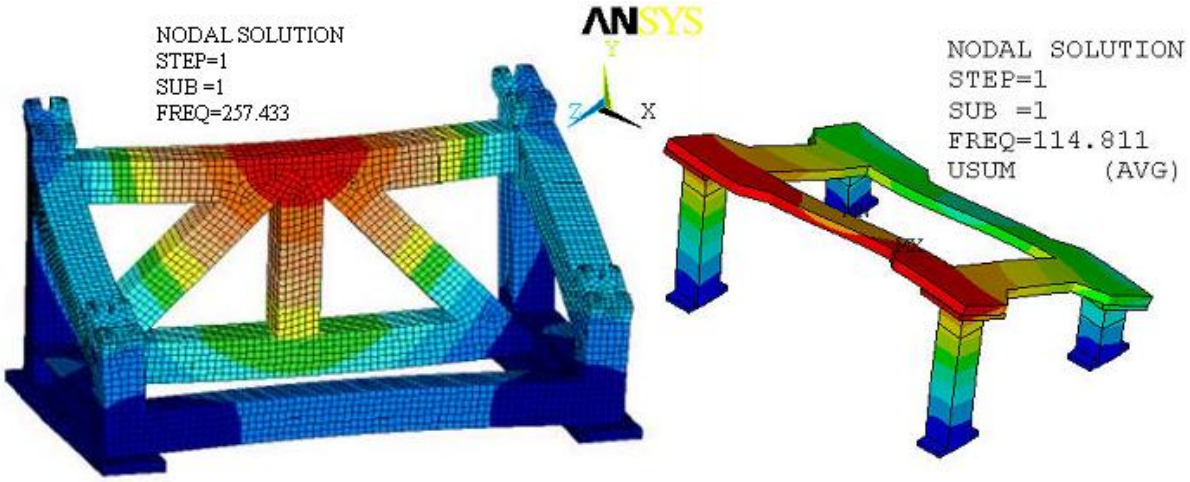

Figure 2.3 First mode of modified and old supporting structure

Figure 2.4 PZT-based production unit with conduit wiring

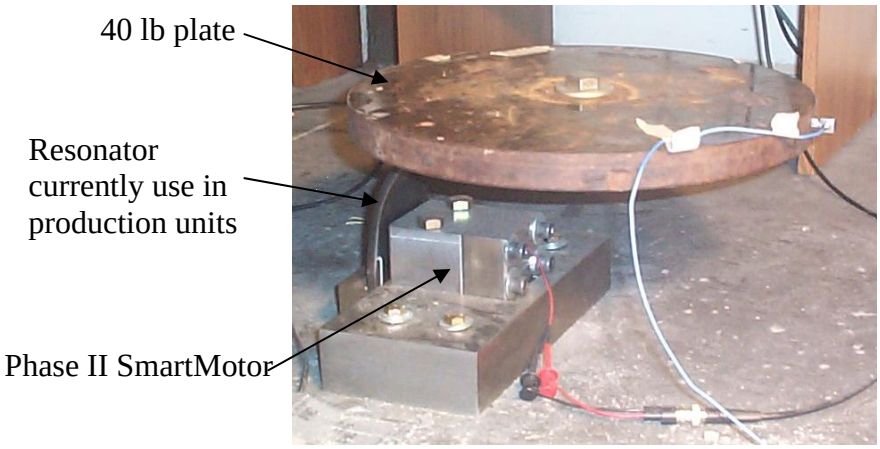

Figure 2.6 Experiment setup used to evaluate PZT based phase II Smart Motor

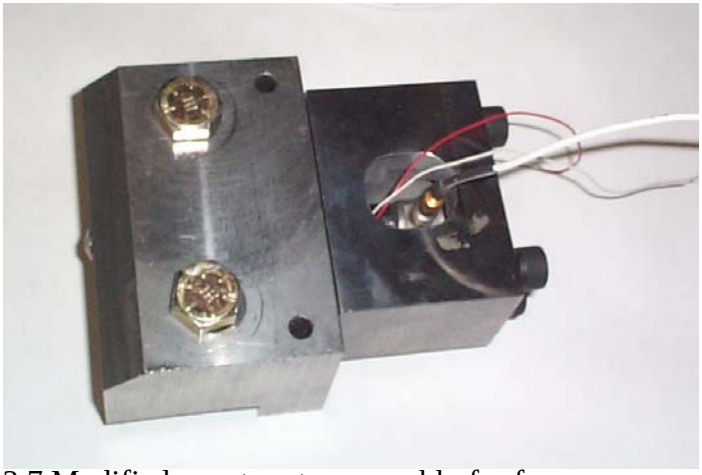

Figure 2.7 Modified smart motor assembly for force measurement

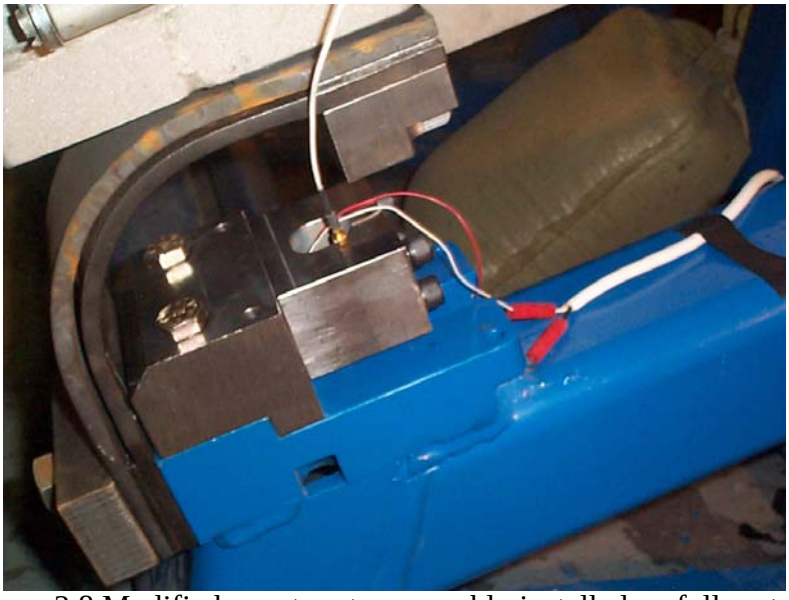

Figure 2.8 Modified smart motor assembly installed on full system

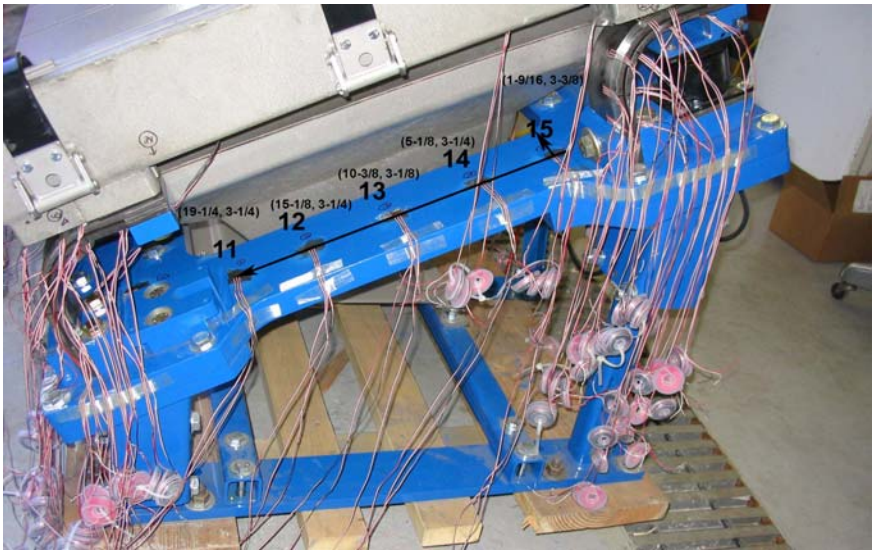

Figure 2.9 Side of S3i 101 with strain gages attached

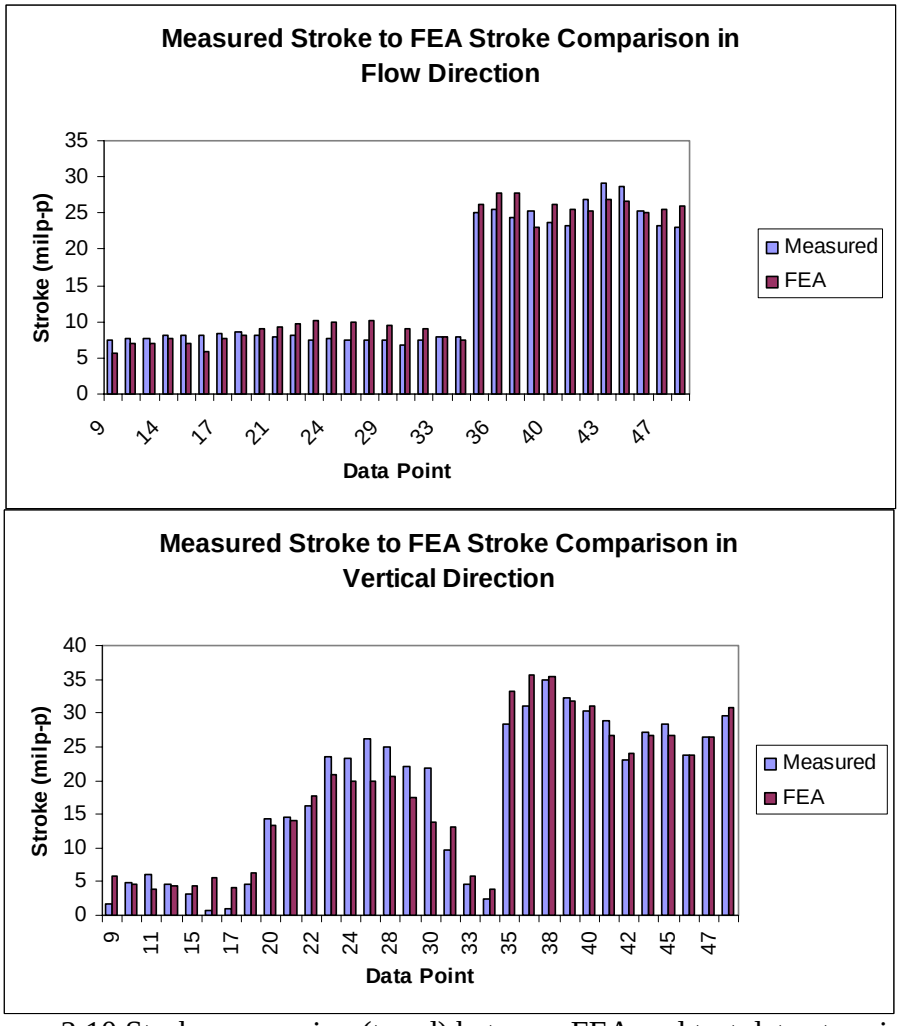

Figure 2.10 Stroke comparing (trend) between FEA and test data at various points on the system (Top: vertical direction, Bottom: flow direction)

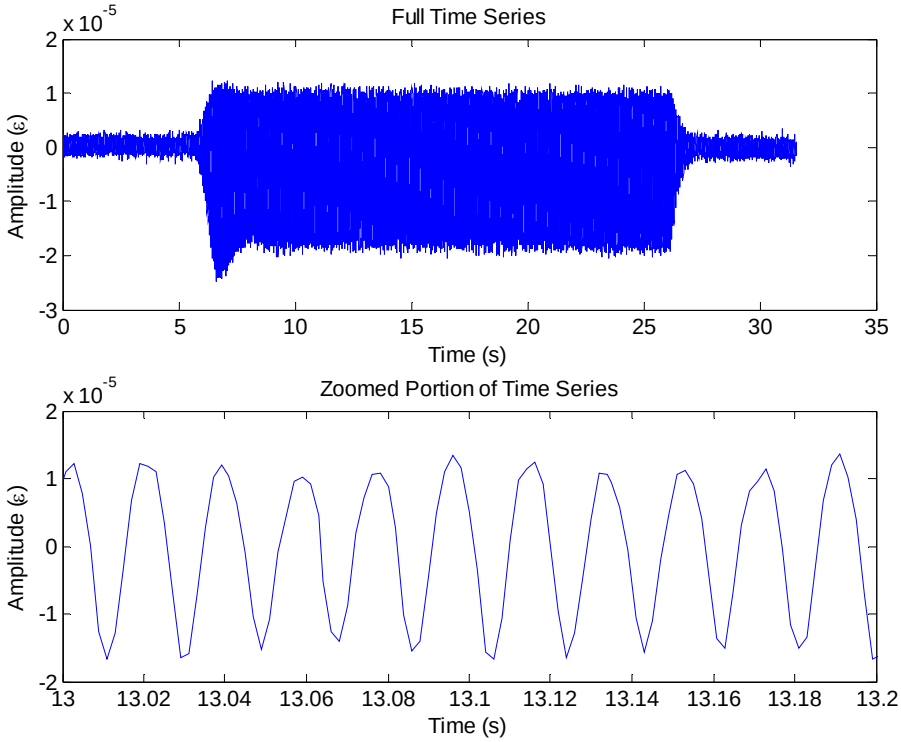

Figure 2.11 Time history from resonator strain gage

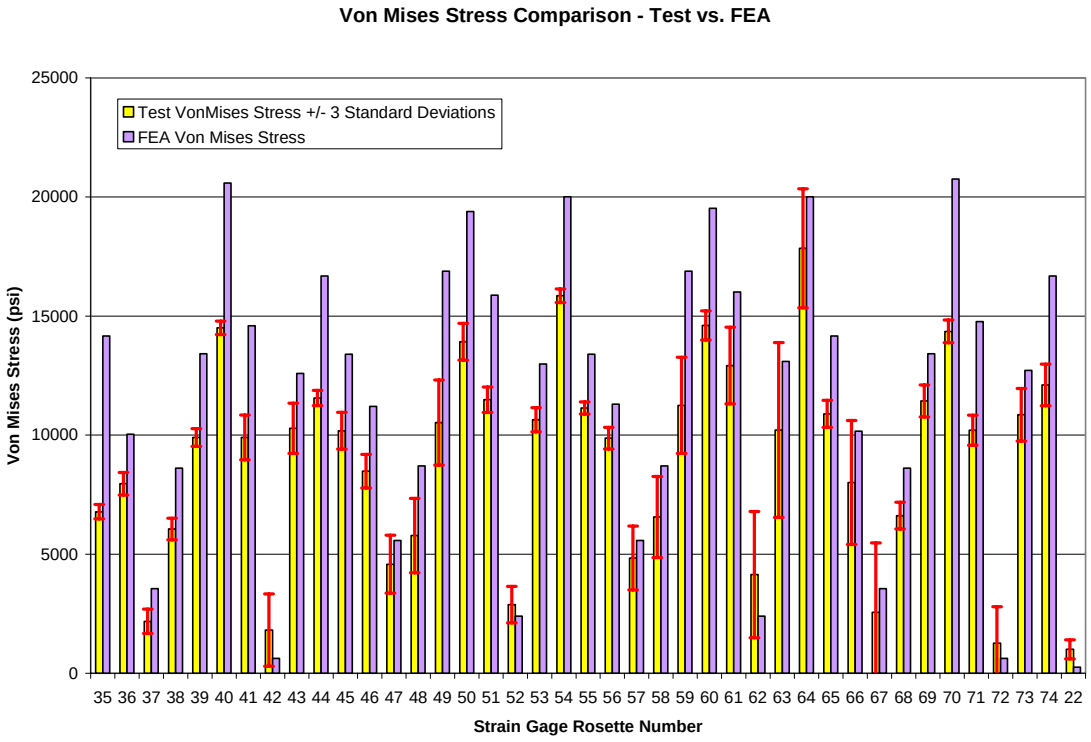

Figure 2.12 Test and FEA Von Mises stress comparison on resonator

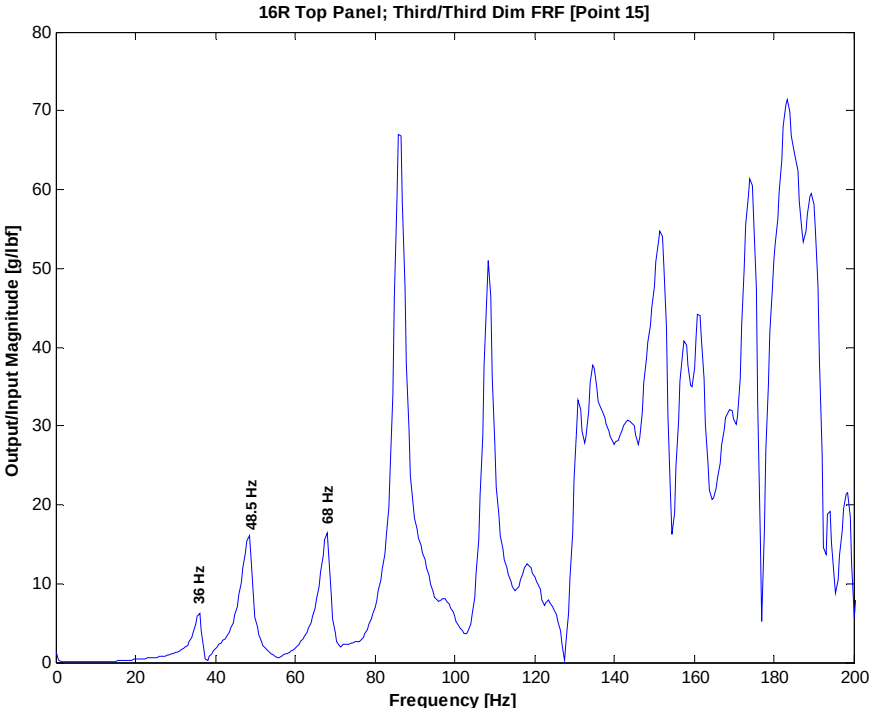

Figure 3.1 Frequency response function of 16R top panel

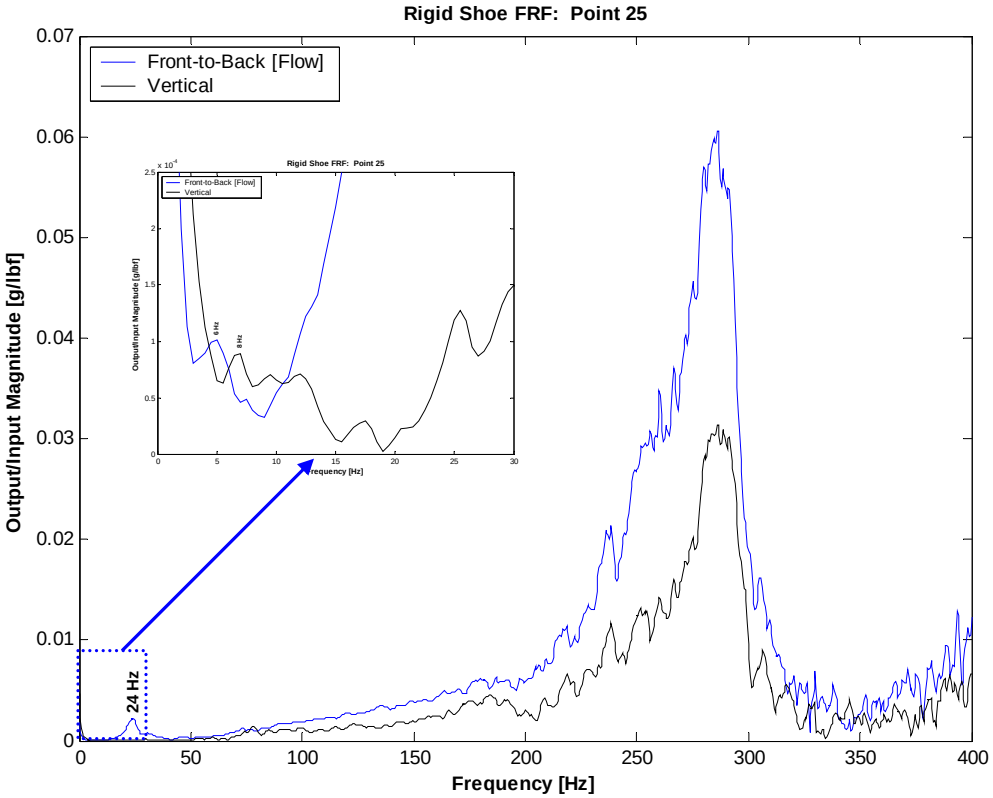

Figure 3.2 Rigid Shoe frequency response function at point 25, vertical and flow directions

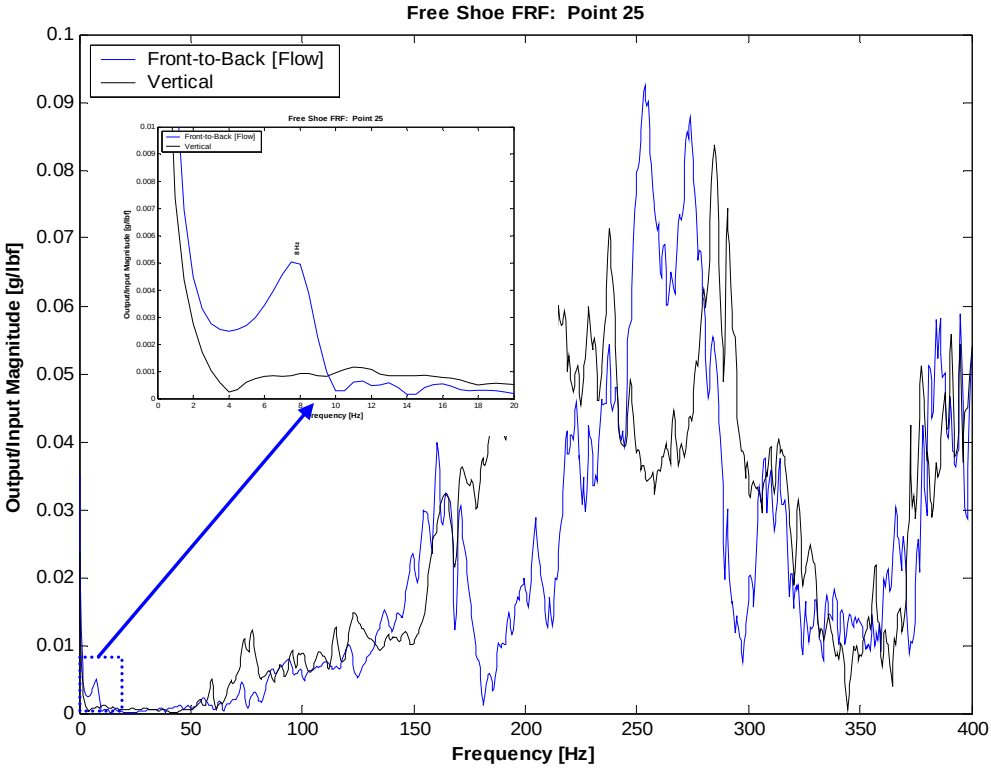

Figure 3.3 Free shoe frequency response function at point 25, vertical & flow directions

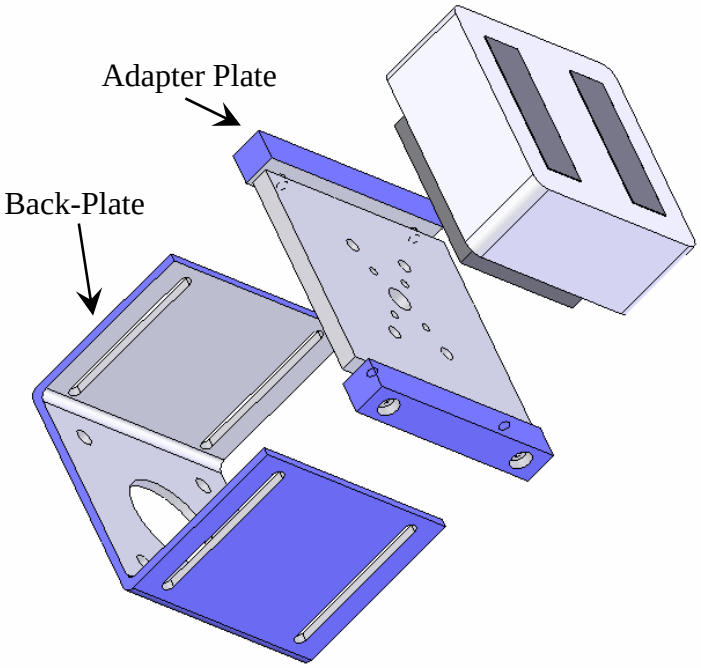

Figure 3.4 Electromagnet drive system design

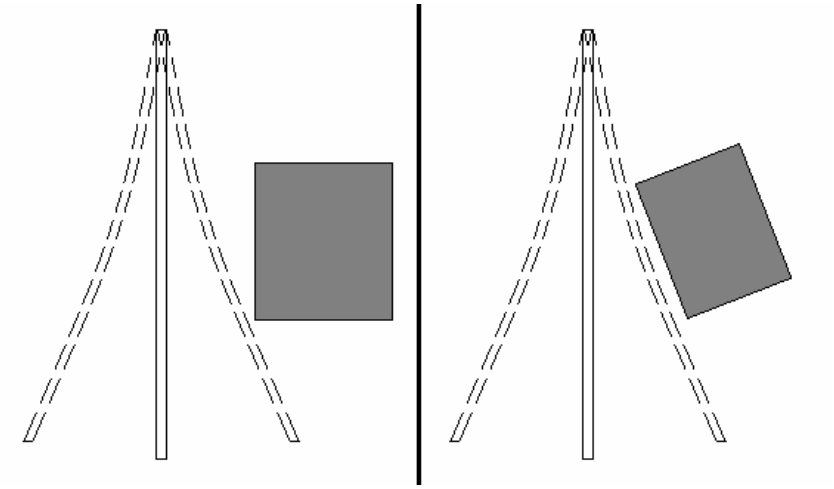

Figure 3.5 Benefit of angled magnet

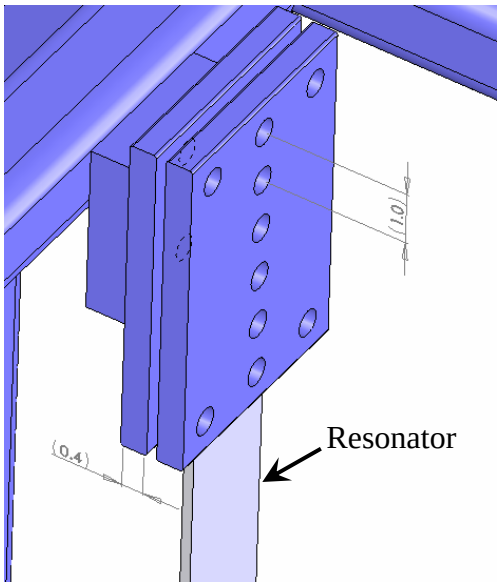

Figure 3.6 System tuning apparatus

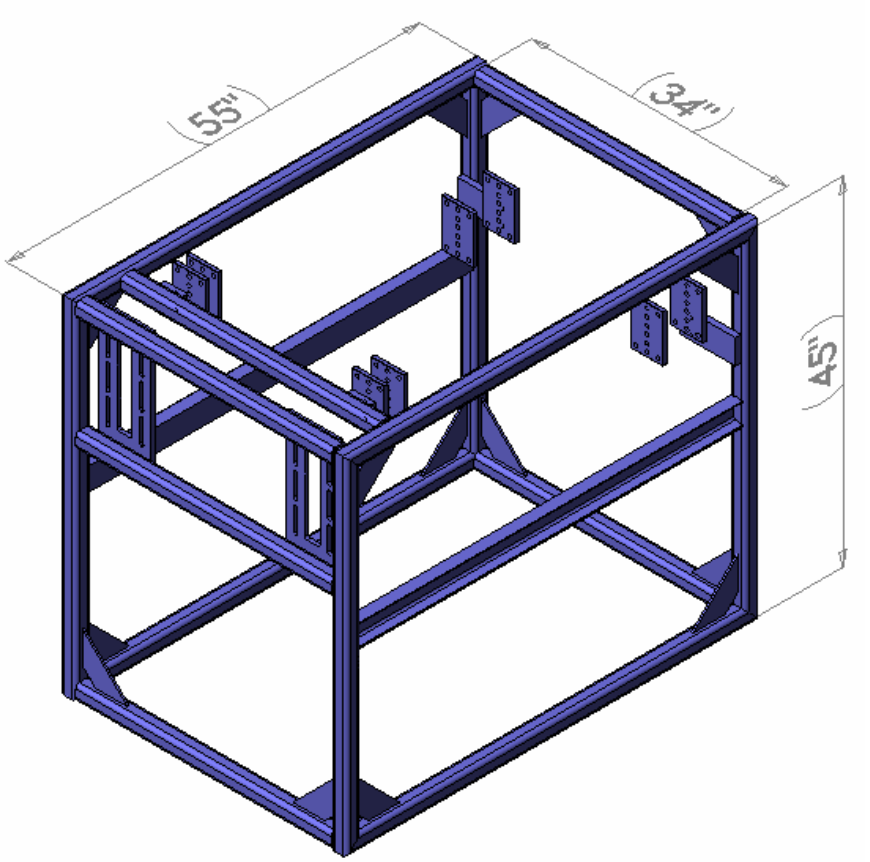

Figure 3.7 System frame design

Figure 5.1 Conventional screening machines with electrical motors and eccentric rotors

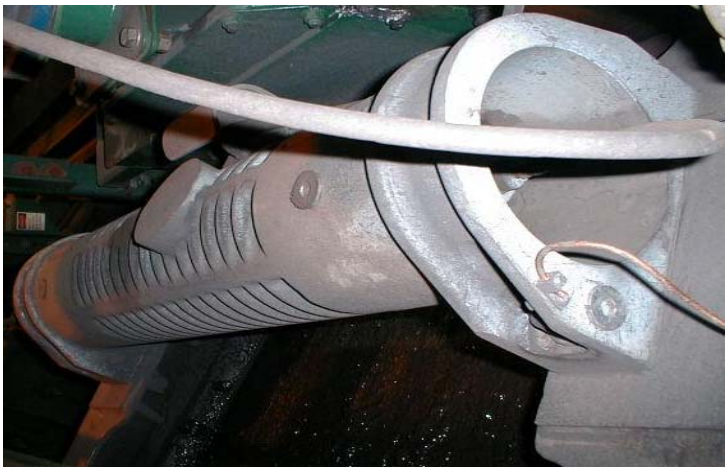

(a)

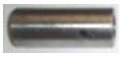

(b)

Figure 5.2 Size Comparison between Smart Motor and conventional motor
(a) conventional eccentric electrical motor (b) PZT-based Smart Motor

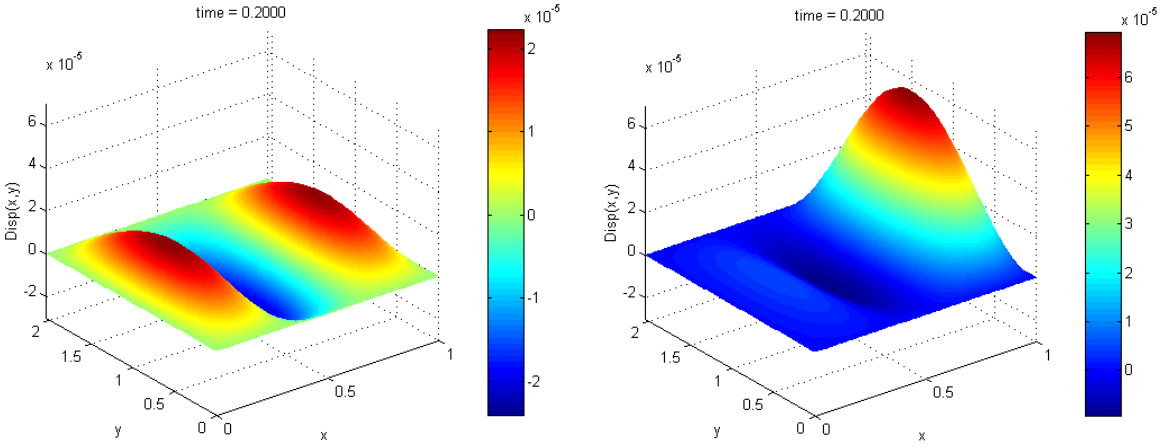

(a) (b)

Figure 5.3 Energy Management Techniques Based on VCC™ and EFC™
(a) unfocused vibratory energy (b) focused vibratory energy

REFERENCES

1. Minntac MTI Grant, New Screen Technology Grant Application, 2001
2. D. J. Tarnowski, D. Allaei, D. Landin, C.P. Chen, and S. Liu, "An Innovative Noise and Vibration Suppression Technique Based on the Combination of Vibration Control by Confinement and Layer Damping Approaches," 3rd Joint Conference – Acoustical Society of America (ASA) and Acoustical Society of Japan (ASJ), Hawaii, 1996.
3. D. Allaei, "Energy-Based Hybrid Vibration Control System for Load-Bearing Skin Structures," Phase I final briefing to Army Space & Missile Defense Command in Huntsville, AL, Paper and CD copy, 1999.
4. D. Allaei, "Energy-Based Hybrid Vibration Control System for Load-Bearing Skin Structures," Final report as part of the MDA Phase I delivered item, 1999.
5. D. Allaei, "Smart Screening System (S3) in Taconite Processing", DOE Project Proposal, 2001.
6. D. Allaei & A. S. Mohammed, "Smart Screening System (S3) in Taconite Processing", semi-annual report I delivered to DOE/NETL, 2003.
7. D. Allaei & A. S. Mohammed, "Smart Screening System (S3) in Taconite Processing", semi-annual report II delivered to DOE/NETL, 2004
8. D. Allaei & A. S. Mohammed, "Smart Screening System (S3) in Taconite Processing", semi-annual report III delivered to DOE/NETL, 2004
9. D. Allaei & A. S. Mohammed, "Smart Screening System (S3) in Taconite Processing", semi-annual report IV delivered to DOE/NETL, 2004
10. D. Allaei & A. S. Mohammed, "Smart Screening System (S3) in Taconite Processing", semi-annual report V delivered to DOE/NETL, 2005
11. D. Allaei & A. Morrison, "Smart Screening System (S3) in Taconite Processing", semi-annual report VI delivered to DOE/NETL, 2005

LIST OF ABBREVIATIONS

S3 – Smart Screen Systems
ARC – Albany Research Center
SM – Smart Motor
SC-S3 – Steering Committee for Smart Screen Systems
PZT – Lead Zirconate Titanate
PMN – Lead Magnesium Niobate
CAD – Computer Aided Design
FEM – Finite Element Analysis
OMS – Operating Mode Shapes
MSHA – Mine Safety and Health Administration's
PLC – Programmable Logic Controller
SPL – Sound Pressure Level
OM – Oscillating Mass
LD – Live Deck
OMR – Oscillating Mass Resonator
CMRL – Coleraine Mineral Research Laboratory, part of The University of Minnesota
IIM – Ispat Inland Mining
SSL-PZT – Suspend Solid Leg PZT System
BPM – Blinding Prevention Mechanism